Energy Conversion and Management 203 (2020) 112243

Contents lists available at ScienceDirect

Energy Conversion and Management

journal homepage: www.elsevier.com/locate/enconman

# A new hybrid algorithm based on grey wolf optimizer and cuckoo search for parameter extraction of solar photovoltaic models

Wen Long[a,b], Shaohong Cai[a,*], Jianjun Jiao[b], Ming Xu[b], Tiebin Wu[c]

[a] Key Laboratory of Economics System Simulation, Guizhou University of Finance and Economics, Guiyang 550025, China
[b] School of Mathematics and Statistics, Guizhou University of Finance and Economics, Guiyang 550025, China
[c] Department of Energy and Electrical Engineering, Hunan University of Humanities, Science and Technology, Loudi 417000, China

ARTICLE INFO

*Keywords:*
Solar photovoltaic model
Parameter extraction
Grey wolf optimizer
Cuckoo search algorithm

ABSTRACT

Quickly, accurately and reliably extract the parameters of solar photovoltaic (PV) model is very critical to simulate, evaluate and control the PV systems. During the past few years, many analytical, numerical and meta-heuristic algorithms have been suggested to extract the parameters of PV models based on the experimental data. However, extracting the parameters of PV models is still a great challenge. In this paper, a new hybrid algorithm based on grey wolf optimizer and cuckoo search (GWOCS) is developed to extract the parameters of different PV cell models with the experimental data under different operating conditions. In GWOCS, a new opposition learning strategy for the decision layer individuals (i.e., $\alpha$, $\beta$, and $\delta$) is proposed to enhance diversity of GWO. The main advantage of GWOCS is its ability to balance between exploration and exploitation. The performance of GWOCS is firstly tested on 10 complex benchmark functions. Then, the GWOCS is applied to extract the parameters of several solar PV cell models under different operating conditions. The comprehensively experimental results show the GWOCS is a promising candidate approach to extract the parameters of solar PV models.

## 1. Introduction

In order to deal with the increasingly serious energy shortage, accelerate adjustment of energy structure and increase research of renewable energy are urgently desired. In recent years, the renewable energy sources such as solar, wind, water, nuclear have received increasing attention [1,2]. Among these renewable energy sources, solar energy is considered as one of the most promising candidates for meeting increasing energy needs. The main type of solar energy is photovoltaic (PV) power generation [3]. However, utilizing PV systems to generate electricity is a great challenge due to their dependence on weather and environmental factors. Therefore, an accurate model that closely representing the nonlinear current-voltage (I-V) characteristics of solar PV cells is required for simulation, evaluation and control of PV systems [4,5]. During the past two decades, many different models have been suggested in the literature to simulate the nonlinear current-voltage characteristics of solar PV cells under different operating conditions. However, the most widely used are the single diode (SD) and double diode (DD) models [6–10]. There are five unknown parameters in SD model and seven unknown parameters in DD model. Accurately and reliably extract these parameters is important to simulate, evaluate and control the solar PV systems. Unfortunately, both SD and DD models are implicit transcendental equations. This implicit property adds a lot of difficulty to the parameters extraction of solar cell and simulation of PV systems. Therefore, it is necessary to suggest an efficient, feasible and reliable approach for accurately extracting the parameters from the current-voltage measurement data of solar PV cells.

In the past few decades, a number of techniques have been suggested in the literature to extract the parameters of solar PV cell models [11]. These existing parameter extraction techniques of solar PV cell models are generally divided into analytical methods and numerical methods. In addition to the appropriate simplifying assumptions, the analytical approaches depend to a large extent on the correctness of several key points on the current-voltage curve, i.e., the open circuit voltage, the short current, the maximum power current, and the maximum power voltage [12–17]. Essentially, the analytical method is “whole participation”, which generalizes all measure current-voltage data using the selected points [8]. If the assignment of the selected point is incorrect, the error of the extracted parameter may be quite significant. Thus, the analytical approaches are often uncertain and bring unsatisfied results in most cases. The numerical approaches use the single point data on the actual current-voltage curve to exactly reproduce the I-V curve. Although this approach is very popular, it

* Corresponding author.
*E-mail address:* gzcd_csh58@126.com (S. Cai).

https://doi.org/10.1016/j.enconman.2019.112243
Received 26 June 2019; Received in revised form 29 October 2019; Accepted 30 October 2019
Available online 09 November 2019
0196-8904/ 

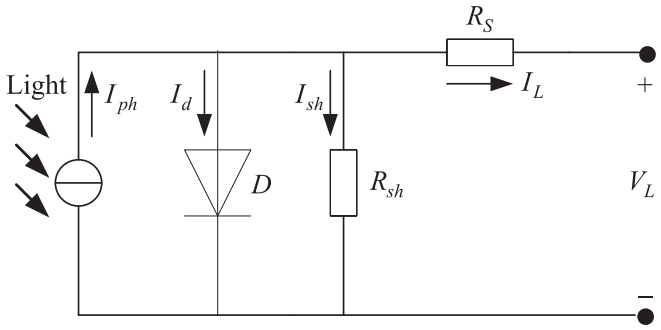


**Fig. 1.** Equivalent circuit of SD model.

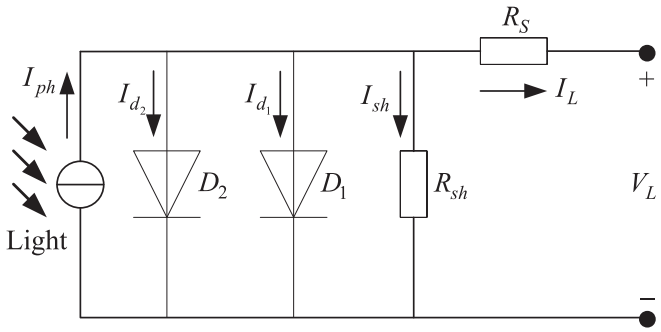


**Fig. 2.** Equivalent circuit of DD model.

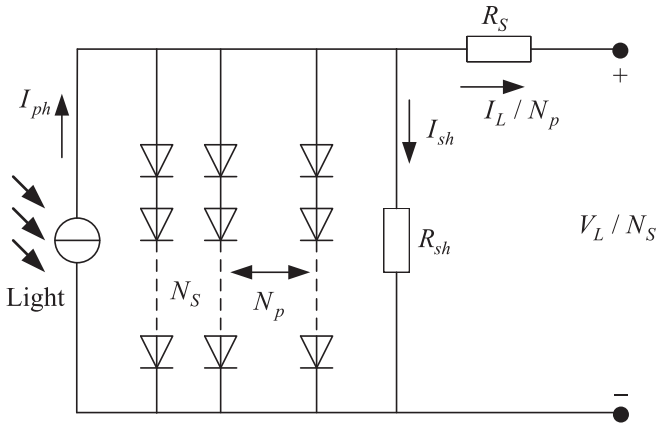


**Fig. 3.** Equivalent circuit of PV panel module model.

consumes all the data points in the I-V curve and complicates the calculation [18,19].

Meta-heuristic algorithms are population-iteration-based global optimization techniques. They impose no restrictions on the problem formulation and have the ability to solve various complex problems. Recently, many meta-heuristic algorithms have been suggested in the literature to extract the parameters of solar PV cell models [20]. They are: genetic algorithm (GA) [21,22], particle swarm optimization (PSO) algorithm [23–25], differential evolution (DE) algorithm [26–28], cuckoo search (CS) algorithm [29], artificial bee colony (ABC) algorithm [30,31], bacterial foraging optimization (BFO) algorithm [11,32,33], biogeography-based optimization (BBO) algorithm [29,34], flower pollination algorithm (FPA) [20,35,36], Jaya optimization (JAYA) algorithm [37,38], salp swarm algorithm (SSA) [39], bird mating optimization (BMO) algorithm [40], teaching-leaning-based optimization (TLBO) algorithm [2,31,41–43], backtracking search algorithm (BSA) [44], whale optimization algorithm (WOA) [27,45], sine cosine algorithm (SCA) [46], imperialist competitive algorithm (ICA) [47], multi-verse optimizer (MVO) algorithm [48], ant lion optimizer

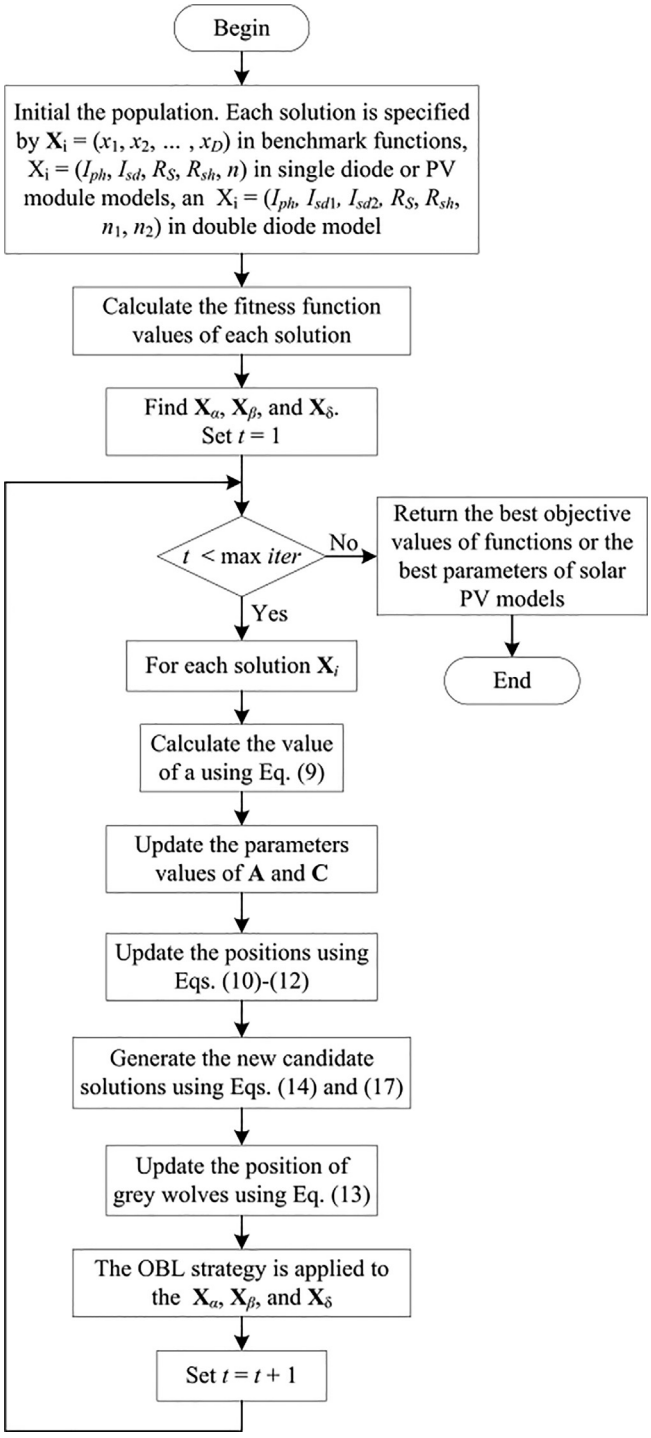


**Fig. 4.** The flow chart of GWOCS algorithm.

(ALO) algorithm [49], cat swarm optimization (CSO) algorithm [50], harmony search (HS) algorithm [51], firefly algorithm (FA) [52], simplified swarm optimization (SSO) algorithm [53], moth-flame optimization (MFO) [54], eagle strategy (ES) [55], water cycle algorithm (WCA) [56,57], shuffled frog leaping (SFL) algorithm [58]. Compared with the analytical and numerical approaches, these meta-heuristic algorithms could obtain satisfactory results for the parameter extraction of PV models. However, these meta-heuristic algorithms still have some inherent disadvantages. For instance, HS is quite sensitive to the initial population. PSO is easily to premature convergence. ABC is poor at exploitation. CS suffers from slow convergence. The performance of DE is depended upon two parameters. Moreover, the performance of these

**Table 1**
Benchmark test functions.

| Function name | Function equation | Search range |
|---|---|---|
| Sphere | $f_1(\boldsymbol{X}) = \sum_{i=1}^{D} x_i^2$ | $[-100, 100]$ |
| Schwefel's 2.22 | $f_2(\boldsymbol{X}) = \sum_{i=1}^{D} \lvert x_i \rvert + \prod_{i=1}^{D} \lvert x_i \rvert$ | $[-10, 10]$ |
| Sum-Square | $f_3(\boldsymbol{X}) = \sum_{i=1}^{D} i\ \ x_i^2$ | $[-10, 10]$ |
| Elliptic | $f_4(\boldsymbol{X}) = \sum_{i=1}^{D} (10^6)^{(i-1)/(n-1)} x_i^2$ | $[-100, 100]$ |
| Ackley | $f_5(\boldsymbol{X}) = -20\exp\left(-0.2\sqrt{\frac{1}{D}\sum_{i=1}^{D} x_i^2}\right) - \exp\left(\frac{1}{D}\sum_{i=1}^{D}\cos(2\pi x_i)\right) + 20 + e$ | $[-32, 32]$ |
| Alpine | $f_6(\boldsymbol{X}) = \sum_{i=1}^{D} \lvert x_i \sin(x_i) + 0.1x_i \rvert$ | $[-10, 10]$ |
| Levy | $f_7(\boldsymbol{X}) = \sum_{i=1}^{D} (x_i - 1)^2[1 + \sin^2(3\pi x_{i+1})] + \sin^2(3\pi x_1) + \lvert x_D - 1 \rvert[1 + \sin^2(3\pi x_D)]$ | $[-10, 10]$ |
| Inverted Cosine Mixture | $f_8(\boldsymbol{X}) = 0.1D - \left(0.1\sum_{i=1}^{D}\cos(5\pi x_i) - \sum_{i=1}^{D} x_i^2\right)$ | $[-1, 1]$ |
| Levy and Montalo | $f_9(\boldsymbol{X}) = 0.1(\sin^2(3\pi x_1) + \sum_{i=1}^{D-1} (x_i - 1)^2(1 + \sin^2(3\pi x_{i+1})) + (x_D - 1)^2(1 + \sin^2(2\pi x_D)))$ | $[-5, 5]$ |
| Stretched V-sine | $f_{10}(\boldsymbol{X}) = \sum_{i=1}^{D-1} (x_i^2 + 2x_{i+1}^2)^{0.25} \cdot ((\sin 50(x_i^2 + x_{i+1}^2)^{0.1})^2 + 1)$ | $[-10, 10]$ |

**Table 2**
Experimental results obtained by four algorithms on 10 test functions.

| Function | GWO | | mGWO | | EGWO | | GWOCS | |
|---|---|---|---|---|---|---|---|---|
| | Mean | St.dev | Mean | St.dev | Mean | St.dev | Mean | St.dev |
| $f_1(x)$ | 1.16E−26 | 3.31E−26 | 4.80E−44 | 1.60E−43 | 7.05E−35 | 1.18E−34 | 0 | 0 |
| $f_2(x)$ | 1.33E−16 | 1.29E−16 | 5.89E−25 | 1.49E−24 | 2.24E−20 | 2.35E−20 | 0 | 0 |
| $f_3(x)$ | 4.51E−28 | 5.36E−28 | 6.21E−44 | 1.69E−43 | 2.73E−34 | 2.91E−34 | 0 | 0 |
| $f_4(x)$ | 2.03E−24 | 2.60E−24 | 7.62E−41 | 1.95E−40 | 2.13E−32 | 2.60E−32 | 0 | 0 |
| $f_5(x)$ | 9.83E−14 | 3.13E−14 | 7.99E−15 | 0 | 6.60E−01 | 1.46E + 00 | 8.88E−16 | 0 |
| $f_6(x)$ | 4.77E−04 | 4.28E−04 | 3.14E−10 | 5.33E−10 | 1.52E + 01 | 3.37E + 00 | 0 | 0 |
| $f_7(x)$ | 5.02E−29 | 4.29E−29 | 9.05E−44 | 1.58E−43 | 3.33E + 02 | 3.68E + 02 | 0 | 0 |
| $f_8(x)$ | 8.88E−17 | 1.99E−16 | 0 | 0 | 0 | 0 | 0 | 0 |
| $f_9(x)$ | 2.73E−30 | 3.70E−30 | 4.64E−47 | 4.16E−47 | 6.82E−38 | 1.38E−37 | 0 | 0 |
| $f_{10}(x)$ | 6.20E−07 | 4.59E−07 | 7.39E−11 | 5.99E−11 | 6.41E + 01 | 1.69E + 01 | 0 | 0 |

**Table 3**
Ranking of the four compared algorithms on 10 benchmark functions according to the Friedman test.

| Algorithm | Friedman ranking | Final ranking |
|---|---|---|
| GWO | 3.60 | 4 |
| mGWO | 2.00 | 2 |
| EGWO | 3.30 | 3 |
| GWOCS | 1.10 | 1 |

meta-heuristic algorithms needs to be strengthened since the parameter extraction problem of PV models is a multimodal optimization problem. Consequently, developing for accurate, reliable and efficient meta-heuristic algorithms to extract the parameters of solar PV cell models is still ongoing.

Recently, hybridization of two meta-heuristic algorithms has been suggested to solve the parameter extraction problem of solar PV models. For example, Ram et al. [20] hybridized ABC with FPA to solve the parameter extraction problem of PV models. Chen and Yu [29] combined CS with BBO and proposed an effectively hybrid meta-heuristic algorithm to extract the parameter of solar PV models. Chen et al. [31] developed a hybrid algorithm by integrating TLBO with ABC for extracting the PV models parameters. Xiong et al. [59] proposed a hybrid algorithm based on DE and WOA for parameter extraction of PV models. Preliminary studies suggested that the hybrid meta-heuristic algorithm achieved better performance than single algorithms on parameter extraction problem of solar PV models.

Grey wolf optimizer (GWO) [60] and cuckoo search (CS) [61] are two widely used meta-heuristic algorithms. However, their search mechanisms are different. GWO is inspired by the hunting behavior of grey wolves and it utilizes three kinds of wolves, i.e., alpha wolf, beta wolf, and delta wolf to search the solution space. CS is inspired by the obligate brood parasitic behavior of cuckoos and it employs Lévy flight to generate new solution. Many studies showed that GWO is good at exploitation [62–64] while CS favors global exploration [65]. To our limited knowledge, hybridizing GWO and CS have not been applied to extract the parameters of solar PV cell models. Therefore, the main goal of this paper is to develop a new parameter extraction method of solar PV cell models (and it is not used to develop a PV parameter extraction technique that can defeat all existing available approaches). The primary contributions of this paper are summarized as follows:

1) A new hybrid algorithm, GWOCS, is developed to extract the parameters of solar PV cell models.
2) GWOCS combined GWO with CS and aims to balance global exploration and local exploitation.
3) The opposition-based learning strategy for the decision layer individuals ($\alpha$, $\beta$, and $\delta$ wolves) is introduced to enhance the diversity of GWO.
4) To fully test the effectiveness of GWOCS, several performance aspects including accuracy, reliability, convergence and statistics are evaluated by using 10 complex benchmark functions and several PV models under different operating conditions.
5) The performance of GWOCS is extensively compared with other parameter extraction techniques in the literature. The results consistently show that GWOCS is a promising candidate technique for extracting the parameters of PV models.

The rest of this paper is organized as follows. Section 2 introduces the PV models and problem formulation. In Section 3, the GWOCS is proposed in detail. Section 4 provides the experimental results and comparisons. Finally, conclusions and future work of this paper are provided in Section 5.

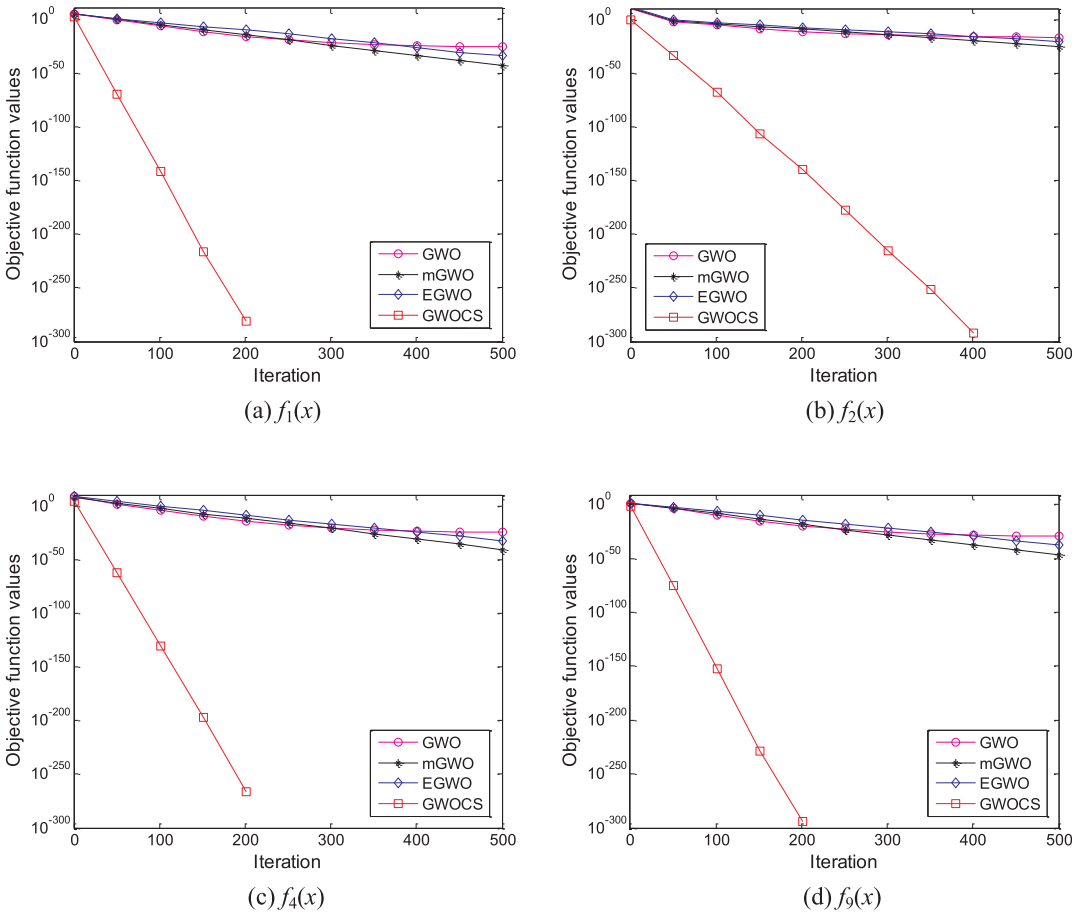


**Fig. 5.** Convergence curves of four typical functions.

**Table 4**
The search range of the parameters for the four PV models.

| Parameter | Single/double diode | | Photowatt-PWP-201 | | STM6-40/36 | |
|---|---|---|---|---|---|---|
| | Lower bound | Upper bound | Lower bound | Upper bound | Lower bound | Upper bound |
| $I_{ph}$ (A) | 0 | 1 | 0 | 2 | 0 | 2 |
| $I_{sd}$, $I_{sd1}$, $I_{sd2}$ (μA) | 0 | 1 | 0 | 50 | 0 | 50 |
| $R_S$ (Ω) | 0 | 0.5 | 0 | 2 | 0 | 0.36 |
| $R_{sh}$ (Ω) | 0 | 100 | 0 | 2000 | 0 | 1000 |
| $n$, $n_1$, $n_2$ | 1 | 2 | 1 | 50 | 1 | 60 |

## 2. PV models and problem formulation

### 2.1. Solar cells

The single diode (SD) model is usually applied to simulate the characteristic of solar cell. The equivalent circuit of SD model is shown in Fig. 1.

In SD model, the output current is computed as follows [29,66]:

$$I_L = I_{ph} - I_d - I_{sh} \tag{1}$$

where $I_L$ represents the output current, $I_{ph}$ denotes the photo generated current, $I_{sh}$ denotes the shunt resistor current, and $I_d$ represents the diode current. Based on Shockley equation, Eq. (1) can be rewritten as follows [66]:

$$I_L = I_{ph} - I_{sd}\cdot\left[\exp\left(\frac{q\cdot(V_L + R_S\cdot I_L)}{n\cdot k\cdot T}\right) - 1\right] - \frac{V_L + R_S\cdot I_L}{R_{sh}} \tag{2}$$

where $I_{sd}$ denotes the reverse saturation current, $V_L$ represents the output voltage, $R_S$ represents the series resistance, $q = 1.60217646 \times 10^{-19}$C denotes the electron charge, $n$ denotes the ideality constant, $R_{sh}$ represents the shunt resistance, $T$ is the cell temperature in Kelvin, and $k = 1.380653 \times 10^{23}$ J/K is the Boltzmann constant.

As can be seen from Eq. (2), in SD model, five parameters (i.e., $I_{ph}$, $I_{sd}$, $R_S$, $R_{sh}$ and $n$) are need to be extracted.

According to [66], the SD model does not consider the effects of recombination current loss in the depletion region. To improve the accuracy of SD model, a double diode (DD) model is obtained when considering the recombination current loss [66]. The equivalent circuit of SD model is shown in Fig. 2.

In DD model, the output current is calculated as follows [29,66]:

$$\begin{aligned} I_L &= I_{ph} - I_{d_1} - I_{d_2} - I_{sh} \\ &= I_{ph} - I_{sd_1}\cdot\left[\exp\left(\tfrac{q\cdot(V_L + R_S\cdot I_L)}{n_1\cdot k\cdot T}\right) - 1\right] - \\ &I_{sd_2}\cdot\left[\exp\left(\tfrac{q\cdot(V_L + R_S\cdot I_L)}{n_2\cdot k\cdot T}\right) - 1\right] - \tfrac{V_L + R_S\cdot I_L}{R_{sh}} \end{aligned} \tag{3}$$

where $I_{d_1}$ and $I_{d_2}$ are the first and second diode currents, $n_1$ and $n_2$ represent the recombination and diffusion diode ideality constants, $I_{sd_1}$ and $I_{sd_2}$ are the saturation and diffusion currents, respectively.

As can be seen from Eq. (3), in DD model, seven parameters (i.e., $I_{ph}$, $I_{sd_1}$, $I_{sd_2}$, $R_S$, $R_{sh}$, $n_1$ and $n_2$) are need to be extracted.

### 2.2. PV panel module model

The equivalent circuit of PV panel module model is shown in Fig. 3. In PV panel module model, the output current is calculated as

**Table 5**
The best extracted parameters and its corresponding RMSE values of various algorithms for single diode model.

| Algorithm | $I_{ph}$ (A) | $I_{sd}$ (μA) | $R_S$ (Ω) | $R_{sh}$ (Ω) | $n$ | RMSE |
|---|---|---|---|---|---|---|
| HISA [19] | 1.032368 | 2.67736 | 1.23178 | 748.4507 | 47.6575 | 2.0166E−03 |
| MADE [28] | 0.7608 | 0.3230 | 0.0364 | 53.7185 | 1.4812 | **9.8602E−04** |
| CS [29] | 0.76048 | 0.36015 | 0.03492 | 43.84232 | 1.4929 | 2.0119E−03 |
| CS-BBO [29] | 0.76078 | 0.32302 | 0.03638 | 53.71852 | 1.48118 | **9.8602E−04** |
| ABC [30] | 0.7608 | 0.3251 | 0.0364 | 53.6433 | 1.4817 | 9.8620E−04 |
| TLBO-ABC [31] | 0.76078 | 0.32302 | 0.03638 | 53.71636 | 1.48118 | **9.8602E−04** |
| BBO-M [34] | 0.76078 | 0.31874 | 0.03642 | 53.36277 | 1.47984 | 9.8634E−04 |
| BLPSO [38] | 0.7607 | 0.36620 | 0.0359 | 60.2845 | 1.4939 | 1.0272E−03 |
| CLPSO [38] | 0.7608 | 0.34302 | 0.0361 | 54.1965 | 1.4873 | 9.9633E−04 |
| BMO [40] | 0.76077 | 0.32479 | 0.03636 | 53.8716 | 1.48173 | **9.8602E−04** |
| GOTLBO [43] | 0.76078 | 0.331552 | 0.036265 | 54.115426 | 1.48382 | 9.8744E−04 |
| IBSA [44] | 0.7607 | 0.35502 | 0.0361 | 58.2012 | 1.4907 | 1.0092E−03 |
| LBSA [44] | 0.7606 | 0.34618 | 0.0362 | 59.0978 | 1.4881 | 1.0143E−03 |
| DE/BBO [44] | 0.7605 | 0.32477 | 0.0364 | 55.2627 | 1.4817 | 9.9922E−04 |
| CWOA [45] | 0.76077 | 0.3239 | 0.03636 | 53.7987 | 1.4812 | **9.8602E−04** |
| ISCA [46] | 0.760778 | 0.323017 | 0.03638 | 53.7182 | 1.4812 | **9.8602E−04** |
| IGHS [51] | 0.76077 | 0.34351 | 0.03613 | 53.2845 | 1.48740 | 9.9306E−04 |
| GGHS [51] | 0.76092 | 0.32620 | 0.03631 | 53.0647 | 1.48217 | 9.9097E−04 |
| PSO-WOA [59] | 0.760563 | 0.340158 | 0.036124 | 59.323133 | 1.486399 | 1.0710E−03 |
| SA [80] | 0.7620 | 0.4798 | 0.0345 | 43.1034 | 1.5172 | 1.7000E−03 |
| GWO | 0.769969 | 0.91215 | 0.02928 | 18.1030 | 1.596658 | 7.5011E−03 |
| mGWO | 0.760595 | 0.38534 | 0.035654 | 64.6624 | 1.49911 | 1.1278E−03 |
| EGWO | 0.763117 | 0.42126 | 0.034838 | 36.1165 | 1.5091 | 2.1121E−03 |
| IGWO | 0.762763 | 0.23878 | 0.036472 | 30.5388 | 1.452148 | 2.3038E−03 |
| AgGWO | 0.769897 | 0.42945 | 0.03306 | 16.8530 | 1.51294 | 6.7762E−03 |
| SCA | 0.7852 | 1.00000 | 0 | 6.25833 | 1.61597 | 4.1410E−02 |
| WOA | 0.7598 | 0.073481 | 0.0421 | 42.77218 | 1.3453 | 3.2001E−03 |
| GWOCS | 0.760773 | 0.32192 | 0.03639 | 53.6320 | 1.4808 | 9.8607E−04 |

**Table 6**
The best extracted parameters and its corresponding RMSE values of various algorithms for double diode model.

| Algorithm | $I_{ph}$ (A) | $I_{sd1}$ (μA) | $I_{sd2}$ (μA) | $R_S$ (Ω) | $R_{sh}$ (Ω) | $n_1$ | $n_2$ | RMSE |
|---|---|---|---|---|---|---|---|---|
| TLBO [2] | 0.7610 | 0.2947 | 0.1373 | 0.0366 | 53.1210 | 1.4730 | 1.9938 | 1.0069E−03 |
| HISA [19] | 1.032368 | 2.64194 | 1.00E−09 | 1.23178 | 748.4507 | 47.6574 | 47.6325 | 2.0166E−03 |
| MADE [28] | 0.7608 | 0.7394 | 0.2246 | 0.03680 | 55.4329 | 1.9963 | 1.4505 | 9.8261E−04 |
| CS [29] | 0.76223 | 0.02732 | 0.50832 | 0.03530 | 97.73242 | 1.70274 | 1.52893 | 2.4440E−03 |
| CS-BBO [29] | 0.76078 | 0.74935 | 0.22597 | 0.03674 | 55.48544 | 2 | 1.45102 | 9.8249E−04 |
| ABC [30] | 0.76071 | 0.14623 | 0.24605 | 0.03654 | 55.36509 | 1.68023 | 1.46226 | 9.8956E−04 |
| TLBO-ABC [31] | 0.76081 | 0.42394 | 0.24011 | 0.03667 | 54.66797 | 1.90750 | 1.45671 | 9.8415E−04 |
| BLPSO [38] | 0.76056 | 0.17895 | 0.31560 | 0.03553 | 64.79937 | 1.69574 | 1.48789 | 1.1042E−03 |
| BMO [40] | 0.76078 | 0.21110 | 0.87688 | 0.03682 | 55.8081 | 1.44533 | 1.99997 | 9.8262E−04 |
| LBSA [44] | 0.7606 | 0.29814 | 0.27096 | 0.0363 | 60.1880 | 1.4760 | 1.9202 | 1.0165E−03 |
| CWOA [45] | 0.76077 | 0.24150 | 0.6 | 0.03666 | 55.2016 | 1.45651 | 1.9899 | 9.8272E−04 |
| ISCA [46] | 0.76078 | 0.74935 | 0.22597 | 0.03674 | 55.48543 | 2 | 1.45102 | **9.8237E−04** |
| IGHS [51] | 0.76079 | 0.97310 | 0.16791 | 0.03690 | 56.8368 | 1.92126 | 1.42814 | 9.8635E−04 |
| PSO-WOA [59] | 0.761091 | 0.20123 | 0.93611 | 0.034223 | 82.82299 | 1.463324 | 1.773674 | 1.6700E−03 |
| SA [80] | 0.7623 | 0.4767 | 0.01 | 0.0345 | 43.1034 | 1.5172 | 2 | 1.9000E−02 |
| GWO | 0.761668 | 0.40302 | 0.45338 | 0.03265 | 72.52775 | 1.6460 | 1.5527 | 2.2124E−03 |
| mGWO | 0.76088 | 0.49333 | 0.17345 | 0.034646 | 62.17868 | 1.52522 | 1.94264 | 1.3163E−03 |
| EGWO | 0.76251 | 0.20856 | 0.12109 | 0.03837 | 32.8813 | 1.6971 | 1.3982 | 1.8062E−03 |
| IGWO | 0.760725 | 0.52878 | 0.23949 | 0.03330 | 80.84466 | 1.5420 | 1.74057 | 1.7576E−03 |
| AgGWO | 0.76003 | 0.30993 | 0.071708 | 0.03643 | 67.6033 | 1.4778 | 1.8839 | 1.1646E−03 |
| SCA | 0.750912 | 0 | 0.94825 | 0 | 7.374536 | 1 | 1.6156 | 4.0585E−02 |
| WOA | 0.761631 | 0.37996 | 0.98043 | 0.029896 | 69.8988 | 1.876598 | 1.609125 | 3.1312E−03 |
| GWOCS | 0.76076 | 0.53772 | 0.24855 | 0.03666 | 54.7331 | 2 | 1.4588 | 9.8334E−04 |

follows [29,66]:

$$I_L/N_p = I_{ph} - I_{sd}\cdot\left[\exp\left(\frac{q\cdot(V_L/N_S + R_S\cdot I_L/N_p)}{n\cdot k\cdot T}\right) - 1\right] - \frac{V_L/N_S + R_S\cdot I_L/N_p}{R_{sh}} \quad (4)$$

where $N_S$ and $N_p$ are the number of solar cells in series and parallel, respectively.

As can be seen from Eq. (4), in PV panel module model, five parameters (i.e., $I_{ph}$, $I_{sd}$, $R_S$, $R_{sh}$ and $n$) are need to be extracted.

### 2.3. Problem formulation

The solar PV model parameter extraction problem is generally transformed into a numerical optimization problem by minimizing the difference between the measured data and simulated ones. The error function is generally defined as the root mean square error (RMSE) as follows [29,56]:

$$\text{RMSE}\ (\text{x}) = \sqrt{\frac{1}{N}\sum_{k=1}^{N} f(V_L,\quad I_L,\quad \text{x})^2} \quad (5)$$

where $N$ denotes the number of measured I-V data.

**Table 7**
The best extracted parameters and its corresponding RMSE values of various algorithms for Photowatt-PWP-201 module model.

| Algorithm | $I_{ph}$ (A) | $I_{sd}$ (μA) | $R_S$ (Ω) | $R_{sh}$ (Ω) | $n$ | RMSE |
|---|---|---|---|---|---|---|
| MADE [28] | 1.0305 | 3.4823 | 1.2013 | 981.9823 | 48.6428 | **2.4251E−03** |
| TLBO-ABC [31] | 1.0305 | 3.4826 | 1.2013 | 982.1815 | 48.6432 | **2.4251E−03** |
| FPA [35] | 1.032091 | 3.047538 | 1.217583 | 811.3721 | 48.13128 | 2.7425E−03 |
| CPSO [36] | 1.0286 | 8.3010 | 1.0755 | 1850.1 | 52.2430 | 3.5000E−03 |
| CLPSO [38] | 1.0304 | 3.6131 | 1.1978 | 1017.0 | 48.7847 | 2.4281E−03 |
| JAYA [38] | 1.0302 | 3.4931 | 1.2014 | 1022.5 | 48.6531 | 2.4278E−03 |
| LBSA [44] | 1.0304 | 3.5233 | 1.2014 | 1020.4 | 48.6866 | 2.4296E−03 |
| MLBSA [44] | 1.0305 | 3.4823 | 1.2013 | 981.9823 | 48.6428 | **2.4251E−03** |
| CWOA [45] | 1.029962 | 3.847725 | 1.201407 | 1172.121142 | 49.023217 | 2.6417E−03 |
| ISCA [46] | 1.030514201 | 3.4822623 | 1.201271659 | 981.9966 | 48.64283 | **2.4251E−03** |
| PSO-WOA [59] | 1.033772 | 3.340338 | 1.205482 | 776.330261 | 48.48701 | 2.6242E−03 |
| SA [80] | 1.0331 | 3.6642 | 1.1989 | 833.3333 | 48.8211 | 2.7000E−03 |
| MPCOA [81] | 1.03188 | 3.3737 | 1.20295 | 849.6927 | 48.50646 | **2.4251E−03** |
| GWO | 1.03038 | 4.9068 | 1.15926 | 1173.7966 | 50 | 2.6749E−03 |
| mGWO | 1.02952 | 4.6005 | 1.17284 | 1261.0638 | 49.7338 | 2.6034E−03 |
| EGWO | 1.02984 | 4.9105 | 1.16042 | 1268.9149 | 50 | 2.6448E−03 |
| IGWO | 1.0277 | 4.9210 | 1.16582 | 1895.9042 | 49.9986 | 2.6228E−03 |
| AgGWO | 1.02808 | 4.9187 | 1.16459 | 1728.7773 | 50 | 2.6145E−03 |
| SCA | 1.0722 | 5.2254 | 1.27171 | 2000 | 50 | 3.1103E−02 |
| WOA | 1.03265 | 2.1278 | 1.22796 | 624.58027 | 46.8347 | 3.6253E−03 |
| GWOCS | 1.03049 | 3.4650 | 1.2019 | 982.7566 | 48.62367 | **2.4251E−03** |

**Table 8**
The best extracted parameters and its corresponding RMSE values of various algorithms for STM6-40/36 module model.

| Algorithm | $I_{ph}$ (A) | $I_{sd}$ (μA) | $R_S$ (Ω) | $R_{sh}$ (Ω) | $n$ | RMSE |
|---|---|---|---|---|---|---|
| TLBO [2] | 1.66248 | 2.63871 | 0.00312 | 19.67204 | 1.56749 | 2.0888E−03 |
| ITLBO [2] | 1.6639 | 1.7387 | 0.0043 | 15.9283 | 1.5203 | **1.7298E−03** |
| MADE [28] | 1.6639 | 1.7387 | 0.0043 | 15.9283 | 1.5203 | **1.7298E−03** |
| CS [29] | 1.66172 | 3.72815 | 0.00173 | 21.74472 | 1.60905 | 2.5159E−03 |
| CS-BBO [29] | 1.6639 | 1.73866 | 0.00427 | 15.92829 | 1.52030 | **1.7298E−03** |
| ABC [30] | 1.65205 | 3.74780 | 0.00247 | 80.12646 | 1.60830 | 5.3510E−03 |
| TLBO-ABC [31] | 1.66317 | 2.14043 | 0.00363 | 17.25952 | 1.54354 | 1.8061E−03 |
| BLPSO [38] | 1.66014 | 6.40784 | 0 | 31.83647 | 1.67848 | 3.6588E−03 |
| GWO | 1.656206 | 7.3440 | 0.00148 | 930.3310 | 1.69641 | 7.1412E−03 |
| mGWO | 1.661132 | 4.3402 | 7.6729E−06 | 19.79153 | 1.62805 | 4.2511E−03 |
| EGWO | 1.686526 | 7.5773 | 0.00277 | 8.54522 | 1.70401 | 1.6458E−02 |
| IGWO | 1.6529 | 1.8956 | 0.005739 | 74.21064 | 1.52897 | 6.3448E−03 |
| AgGWO | 1.6719 | 4.2897 | 0 | 11.49035 | 1.62750 | 5.8391E−03 |
| SCA | 1.657516 | 4.2608 | 0 | 365.10478 | 1.62971 | 2.5407E−02 |
| WOA | 1.6800 | 0.49760 | 0.00618 | 7.2316 | 1.39497 | 7.5211E−03 |
| GWOCS | 1.6641 | 1.7449 | 0.00424 | 15.7326 | 1.5207 | 1.7337E−03 |

In Eq. (5), for SD model,

$$\begin{cases} f(V_L, I_L, \mathrm{x}) = I_{ph} - I_{sd}\cdot\left[\exp\left(\frac{q\cdot(V_L + R_S\cdot I_L)}{n\cdot k\cdot T}\right) - 1\right] - \frac{V_L + R_S\cdot I_L}{R_{sh}} - I_L \\ \mathrm{x}=\{I_{ph}, I_{sd}, R_S, R_{sh}, n\} \end{cases} \tag{6}$$

For DD model,

$$\begin{cases} f(V_L, I_L, \mathrm{x}) = I_{ph} - I_{sd_1}\cdot\left[\exp\left(\frac{q\cdot(V_L + R_S\cdot I_L)}{n_1\cdot k\cdot T}\right) - 1\right] - I_{sd_2}\cdot \\ \qquad\left[\exp\left(\frac{q\cdot(V_L + R_S\cdot I_L)}{n_2\cdot k\cdot T}\right) - 1\right] - \frac{V_L + R_S\cdot I_L}{R_{sh}} - I_L \\ \mathrm{x}=\{I_{ph}, I_{sd_1}, I_{sd_2}, R_S, R_{sh}, n_1, n_2\} \end{cases} \tag{7}$$

## 3. Hybrid GWO and CS algorithm

### 3.1. Grey wolf optimizer

Grey wolf optimizer (GWO) [60] is a new developed meta-heuristic algorithm which simulates the hunting behavior of wolves swarm. In GWO, the best individual is called $\alpha$ wolf, the second- and third-best individuals are named as $\beta$ and $\delta$ wolves, respectively, and the other individuals are called as $\omega$ wolves. The behavior of the wolf swarm encircling the prey is modeled as follows [60]:

$$\boldsymbol{X}(t+1) = \boldsymbol{X}_p(t) - \boldsymbol{A}\cdot|\boldsymbol{C}\cdot\boldsymbol{X}_p(t) - \boldsymbol{X}(t)| \tag{8}$$

where $\boldsymbol{X}$ represents the position vector of wolf, $t$ denotes the number of iterations, $\mathbf{X}_p$ is the position vector of prey, $\boldsymbol{A} = 2\cdot\boldsymbol{a}\times\boldsymbol{r}_1 - \boldsymbol{a}$ and $\boldsymbol{C} = 2\times\boldsymbol{r}_2$ are coefficient, $r_1 \in [0, 1]$ and $r_2 \in [0, 1]$ are random number, and $\boldsymbol{a}$ is calculated as follows:

$$\boldsymbol{a}(t) = 2 - \frac{2t}{\max iter} \tag{9}$$

where $\max iter$ is the maximum number of iterations.

The positions of the other individuals in the population are updated by $\alpha$, $\beta$ and $\delta$ wolves as follows:

$$\boldsymbol{X}_1 = \boldsymbol{X}_\alpha - \boldsymbol{A}_1\cdot|\boldsymbol{C}_1\cdot\boldsymbol{X}_\alpha - \boldsymbol{X}| \tag{10}$$

$$\boldsymbol{X}_2 = \boldsymbol{X}_\beta - \boldsymbol{A}_2\cdot|\boldsymbol{C}_2\cdot\boldsymbol{X}_\beta - \boldsymbol{X}| \tag{11}$$

$$\boldsymbol{X}_3 = \boldsymbol{X}_\delta - \boldsymbol{A}_3\cdot|\boldsymbol{C}_3\cdot\boldsymbol{X}_\delta - \boldsymbol{X}| \tag{12}$$

$$\boldsymbol{X}(t+1) = \frac{\boldsymbol{X}_1(t) + \boldsymbol{X}_2(t) + \boldsymbol{X}_3(t)}{3} \tag{13}$$

where $\boldsymbol{A}_1$, $\boldsymbol{A}_2$, and $\boldsymbol{A}_3$ are similar to $\boldsymbol{A}$, $\boldsymbol{C}_1$, $\boldsymbol{C}_2$, and $\boldsymbol{C}_3$ are similar to $\boldsymbol{C}$.

**Table 9**
The calculated values of current and power and IAE obtained by GWOCS for the single diode model.

| Item | $V_L$ (V) | $I_L$ measured (A) | $I_L$ calculated (A) | IAE ($I_L$) | $P_L$ measured (W) | $P_L$ calculated (W) | IAE ($P_L$) |
|---|---|---|---|---|---|---|---|
| 1 | −0.2057 | 0.7640 | 0.764090298 | 0.00009030 | −0.1571548 | −0.15717337 | 0.00001857 |
| 2 | −0.1291 | 0.7620 | 0.762662998 | 0.00066300 | −0.0983742 | −0.09845979 | 0.00008559 |
| 3 | −0.0588 | 0.7605 | 0.761352996 | 0.00085299 | −0.0447174 | −0.04476756 | 0.00005016 |
| 4 | 0.0057 | 0.7605 | 0.760150660 | 0.00034934 | 0.00433485 | 0.004332859 | 0.00000199 |
| 5 | 0.0646 | 0.7600 | 0.759080944 | 0.00094906 | 0.04909600 | 0.049034691 | 0.00006131 |
| 6 | 0.1185 | 0.7590 | 0.758035964 | 0.00096404 | 0.08994150 | 0.089827262 | 0.00011424 |
| 7 | 0.1678 | 0.7570 | 0.757083132 | 0.00008313 | 0.12702460 | 0.127038550 | 0.00001395 |
| 8 | 0.2132 | 0.7570 | 0.756132419 | 0.00086758 | 0.16139240 | 0.161207432 | 0.00018497 |
| 9 | 0.2545 | 0.7555 | 0.755076823 | 0.00042318 | 0.19227475 | 0.192167051 | 0.00010770 |
| 10 | 0.2924 | 0.7540 | 0.753653643 | 0.00034636 | 0.22046960 | 0.220368325 | 0.00101275 |
| 11 | 0.3269 | 0.7505 | 0.751377703 | 0.00087770 | 0.24533845 | 0.245625371 | 0.00028692 |
| 12 | 0.3585 | 0.7465 | 0.747339560 | 0.00083956 | 0.26762025 | 0.267921232 | 0.00030098 |
| 13 | 0.3873 | 0.7385 | 0.740090966 | 0.00159097 | 0.28602105 | 0.286637231 | 0.00061618 |
| 14 | 0.4137 | 0.7280 | 0.727395041 | 0.00060496 | 0.30117360 | 0.300923328 | 0.00025027 |
| 15 | 0.4373 | 0.7065 | 0.706956635 | 0.00045663 | 0.30895245 | 0.309152137 | 0.00019969 |
| 16 | 0.4590 | 0.6755 | 0.675301516 | 0.00019848 | 0.31005450 | 0.309963396 | 0.00009110 |
| 17 | 0.4784 | 0.6320 | 0.630893171 | 0.00110683 | 0.30234880 | 0.301819293 | 0.00052951 |
| 18 | 0.4960 | 0.5730 | 0.572090876 | 0.00090912 | 0.28420800 | 0.283757075 | 0.00045093 |
| 19 | 0.5119 | 0.4990 | 0.499498403 | 0.00049840 | 0.25543810 | 0.255693233 | 0.00025513 |
| 20 | 0.5365 | 0.4130 | 0.413497286 | 0.00049728 | 0.21744450 | 0.217706321 | 0.00026182 |
| 21 | 0.5398 | 0.3165 | 0.317220561 | 0.00072056 | 0.17084670 | 0.171235659 | 0.00038896 |
| 22 | 0.5521 | 0.2120 | 0.212103089 | 0.00010309 | 0.11704520 | 0.117102115 | 0.00005692 |
| 23 | 0.5633 | 0.1035 | 0.102722418 | 0.00077758 | 0.05830155 | 0.057863538 | 0.00043801 |
| 24 | 0.5736 | −0.0100 | −0.00924405 | 0.00075595 | −0.0057360 | −0.00530239 | 0.00043361 |
| 25 | 0.5833 | −0.1230 | −0.12437012 | 0.00137012 | −0.0717459 | −0.07254509 | 0.00079919 |
| 26 | 0.5900 | −0.2100 | −0.20917550 | 0.00082449 | −0.1239000 | −0.12341355 | 0.00048645 |

**Table 10**
The calculated values of current and power and IAE obtained by GWOCS for the double diode model.

| Item | $V_L$ (V) | $I_L$ measured (A) | $I_L$ calculated (A) | IAE ($I_L$) | $P_L$ measured (W) | $P_L$ calculated (W) | IAE ($P_L$) |
|---|---|---|---|---|---|---|---|
| 1 | −0.2057 | 0.7640 | 0.764011633 | 0.00001696 | −0.1571548 | −0.15715719 | 0.00000239 |
| 2 | −0.1291 | 0.7620 | 0.762612979 | 0.00059756 | −0.0983742 | −0.09845334 | 0.00007915 |
| 3 | −0.0588 | 0.7605 | 0.761329147 | 0.00079481 | −0.0447174 | −0.04476615 | 0.00004875 |
| 4 | 0.0057 | 0.7605 | 0.760150437 | 0.00040087 | 0.00433485 | 0.004332857 | 0.00000199 |
| 5 | 0.0646 | 0.7600 | 0.759071358 | 0.00099450 | 0.04909600 | 0.049036010 | 0.00005999 |
| 6 | 0.1185 | 0.7590 | 0.758072606 | 0.00100387 | 0.08994150 | 0.089831604 | 0.00010989 |
| 7 | 0.1678 | 0.7570 | 0.757130336 | 0.00004849 | 0.12702460 | 0.127046470 | 0.00002187 |
| 8 | 0.2132 | 0.7570 | 0.756181648 | 0.00089725 | 0.16139240 | 0.161217927 | 0.00017447 |
| 9 | 0.2545 | 0.7555 | 0.755116634 | 0.00044793 | 0.19227475 | 0.192177183 | 0.00009756 |
| 10 | 0.2924 | 0.7540 | 0.753670914 | 0.00036586 | 0.22046960 | 0.220373375 | 0.00009622 |
| 11 | 0.3269 | 0.7505 | 0.751361238 | 0.00086416 | 0.24533845 | 0.245619989 | 0.00028154 |
| 12 | 0.3585 | 0.7465 | 0.747285020 | 0.00083315 | 0.26762025 | 0.267901680 | 0.00028143 |
| 13 | 0.3873 | 0.7385 | 0.740006601 | 0.00159294 | 0.28602105 | 0.286604556 | 0.00058351 |
| 14 | 0.4137 | 0.7280 | 0.727303430 | 0.00059386 | 0.30117360 | 0.300885429 | 0.00028817 |
| 15 | 0.4373 | 0.7065 | 0.706888873 | 0.00047596 | 0.30895245 | 0.309122504 | 0.00017005 |
| 16 | 0.4590 | 0.6755 | 0.675284893 | 0.00017357 | 0.31005450 | 0.309955766 | 0.00009873 |
| 17 | 0.4784 | 0.6320 | 0.630935619 | 0.00108065 | 0.30234880 | 0.301839600 | 0.00050920 |
| 18 | 0.4960 | 0.5730 | 0.572177860 | 0.00088583 | 0.28420800 | 0.283800218 | 0.00040778 |
| 19 | 0.5119 | 0.4990 | 0.499599725 | 0.00051674 | 0.25543810 | 0.255745099 | 0.00030700 |
| 20 | 0.5365 | 0.4130 | 0.413581487 | 0.00051184 | 0.21744450 | 0.217750653 | 0.00030615 |
| 21 | 0.5398 | 0.3165 | 0.317267102 | 0.00073592 | 0.17084670 | 0.171260782 | 0.00041408 |
| 22 | 0.5521 | 0.2120 | 0.212107429 | 0.00012636 | 0.11704520 | 0.117104512 | 0.00005931 |
| 23 | 0.5633 | 0.1035 | 0.102696245 | 0.00073824 | 0.05830155 | 0.057848795 | 0.00045276 |
| 24 | 0.5736 | −0.0100 | −0.00927853 | 0.00081954 | −0.0057360 | −0.00532216 | 0.00041384 |
| 25 | 0.5833 | −0.1230 | −0.12438421 | 0.00127408 | −0.0717459 | −0.07255331 | 0.00080741 |
| 26 | 0.5900 | −0.2100 | −0.20915459 | 0.00094888 | −0.1239000 | −0.12340121 | 0.00049879 |

### 3.2. Cuckoo search

Cuckoo search (CS) [61] is a widely used meta-heuristics algorithm which mimics the breeding parasitism behavior of cuckoos. In CS, a solution corresponds to a cuckoo egg. During the process of iterative, the new candidate solution is generated by Lévy flight as follows [61]:

$$\begin{aligned} \boldsymbol{X}_i &= \boldsymbol{X}_i - \gamma\cdot(\boldsymbol{X}_i - \boldsymbol{X}_{\mathrm{g}})\oplus \mathrm{Levy}(\lambda) \\ &= \boldsymbol{X}_i + \frac{0.01u}{|v|^{1/\lambda}}(\boldsymbol{X}_i - \boldsymbol{X}_{\mathrm{g}}) \end{aligned} \tag{14}$$

where $\boldsymbol{X}_i$ is the $i$-th solution, $\gamma > 0$ is the step scaling size, $\boldsymbol{X}_g$ is the global optimal solution, $\oplus$ represents the entry-wise multiplications, $\lambda$ is the Lévy flight exponent, $u$ and $v$ are random numbers respectively and they are satisfied with normal distribution [61]:

$$u\tilde{\mathrm{N}}(0,\ \sigma_u^2),\ v\tilde{\mathrm{N}}(0,\ \sigma_v^2) \tag{15}$$

$$\sigma_u = \left[\frac{\sin(\lambda\pi/2)\cdot\Gamma(1+\lambda)}{2^{(\lambda-1)/2}\lambda\cdot\Gamma\left(\frac{1+\lambda}{2}\right)}\right]^{1/\lambda},\quad \sigma_v = 1 \tag{16}$$

where $\Gamma(\cdot)$ represents the Gamma function.

Moreover, CS also utilizes the discovery operator to replace the discovered nests with probability $p_a$ as follows [61]:

**Table 11**
The calculated values of current and power and IAE obtained by GWOCS for the Photowatt-PWP-201 module model.

| Item | $V_L$ (V) | $I_L$ measured (A) | $I_L$ calculated (A) | IAE ($I_L$) | $P_L$ measured (W) | $P_L$ calculated (W) | IAE ($P_L$) |
|---|---|---|---|---|---|---|---|
| 1 | 0.1248 | 1.0315 | 1.02909403 | 0.00240597 | 0.1287312 | 0.128430935 | 0.00030026 |
| 2 | 1.8093 | 1.0300 | 1.02735773 | 0.00264227 | 1.8635790 | 1.858798345 | 0.00478065 |
| 3 | 3.3511 | 1.0260 | 1.02571698 | 0.00028302 | 3.4382286 | 3.437280185 | 0.00094842 |
| 4 | 4.7622 | 1.0220 | 1.02408051 | 0.00208051 | 4.8669684 | 4.876876220 | 0.00990782 |
| 5 | 6.0538 | 1.0180 | 1.02226211 | 0.00426211 | 6.1627684 | 6.188570362 | 0.02580196 |
| 6 | 7.2364 | 1.0155 | 1.01989919 | 0.00439919 | 7.3485642 | 7.380398532 | 0.03183433 |
| 7 | 8.3189 | 1.0140 | 1.01633705 | 0.00233705 | 8.4353646 | 8.454806273 | 0.01944167 |
| 8 | 9.3097 | 1.0100 | 1.01048363 | 0.00048363 | 9.4027970 | 9.407299506 | 0.00450251 |
| 9 | 10.2163 | 1.0035 | 1.00067843 | 0.00282156 | 10.252057 | 10.22323111 | 0.02882594 |
| 10 | 11.0449 | 0.9880 | 0.98466286 | 0.00333714 | 10.912361 | 10.87550280 | 0.03685840 |
| 11 | 11.8018 | 0.9630 | 0.95971512 | 0.00328487 | 11.365133 | 11.32636595 | 0.03876745 |
| 12 | 12.4929 | 0.9255 | 0.92307310 | 0.00242690 | 11.562179 | 11.53185997 | 0.03031898 |
| 13 | 13.1231 | 0.8725 | 0.87261492 | 0.00011492 | 11.449905 | 11.45141283 | 0.00150808 |
| 14 | 13.6983 | 0.8075 | 0.80733425 | 0.00016575 | 11.061377 | 11.05910672 | 0.00227053 |
| 15 | 14.2221 | 0.7265 | 0.72797504 | 0.00147504 | 10.332355 | 10.35333383 | 0.02097818 |
| 16 | 14.6995 | 0.6345 | 0.63647421 | 0.00197421 | 9.3268327 | 9.355852572 | 0.02901982 |
| 17 | 15.1346 | 0.5345 | 0.53569493 | 0.00119493 | 8.0894437 | 8.107528547 | 0.01808485 |
| 18 | 15.5311 | 0.4275 | 0.42880780 | 0.00130780 | 6.6395452 | 6.659856838 | 0.02031159 |
| 19 | 15.8929 | 0.3185 | 0.31865622 | 0.00015622 | 5.0618886 | 5.064371457 | 0.00248281 |
| 20 | 16.2229 | 0.2085 | 0.20784417 | 0.00065583 | 3.3824746 | 3.371835140 | 0.01063951 |
| 21 | 16.5241 | 0.1010 | 0.09834425 | 0.00265575 | 1.6689341 | 1.625050222 | 0.04388388 |
| 22 | 16.7987 | −0.008 | −0.0081732 | 0.00017322 | −0.134390 | −0.13729947 | 0.00290987 |
| 23 | 17.0499 | −0.111 | −0.1109637 | 0.00003631 | −1.892539 | −1.89191980 | 0.00061910 |
| 24 | 17.2793 | −0.209 | −0.2091022 | 0.00010220 | −3.611374 | −3.61813959 | 0.00176589 |
| 25 | 17.4885 | −0.303 | −0.3019949 | 0.00100513 | −5.299016 | −5.28143730 | 0.01757820 |

**Table 12**
The calculated values of current and power and IAE obtained by GWOCS for the STM6-40/36 module model.

| Item | $V_L$ (V) | $I_L$ measured (A) | $I_L$ calculated (A) | IAE ($I_L$) | $P_L$ measured (W) | $P_L$ calculated (W) | IAE ($P_L$) |
|---|---|---|---|---|---|---|---|
| 1 | 0 | 1.663 | 1.66363602 | 0.00063602 | 0 | 0 | 0 |
| 2 | 0.118 | 1.663 | 1.66342757 | 0.00042757 | 0.196234 | 0.196284453 | 0.00005045 |
| 3 | 2.237 | 1.661 | 1.65968058 | 0.00131942 | 3.715657 | 3.712705449 | 0.00295155 |
| 4 | 5.434 | 1.653 | 1.65397455 | 0.00097455 | 8.982402 | 8.987697698 | 0.00529570 |
| 5 | 7.260 | 1.650 | 1.65058644 | 0.00058644 | 11.97900 | 11.98325752 | 0.00425752 |
| 6 | 9.680 | 1.645 | 1.64539768 | 0.00039768 | 15.92360 | 15.92744955 | 0.00384955 |
| 7 | 11.59 | 1.640 | 1.63915938 | 0.00084062 | 19.00760 | 18.99785718 | 0.00974282 |
| 8 | 12.60 | 1.636 | 1.63361872 | 0.00238128 | 20.61360 | 20.58359587 | 0.03000413 |
| 9 | 13.37 | 1.629 | 1.62717642 | 0.00182358 | 21.77973 | 21.75534869 | 0.02438131 |
| 10 | 14.09 | 1.619 | 1.61818996 | 0.00081004 | 22.81171 | 22.80029560 | 0.01141350 |
| 11 | 14.88 | 1.597 | 1.60293106 | 0.00593106 | 23.76336 | 23.85161422 | 0.08825422 |
| 12 | 15.59 | 1.581 | 1.58144417 | 0.00044417 | 24.64779 | 24.65471467 | 0.00692467 |
| 13 | 16.40 | 1.542 | 1.54219273 | 0.00019273 | 25.28880 | 25.29196075 | 0.00316075 |
| 14 | 16.71 | 1.524 | 1.52109732 | 0.00290268 | 25.46604 | 25.41753615 | 0.04850385 |
| 15 | 16.98 | 1.500 | 1.49908700 | 0.00091300 | 25.47000 | 25.45449725 | 0.01550275 |
| 16 | 17.13 | 1.485 | 1.48515866 | 0.00015866 | 25.43805 | 25.44076782 | 0.00271782 |
| 17 | 17.32 | 1.465 | 1.46554005 | 0.00054005 | 25.37380 | 25.38315369 | 0.00935369 |
| 18 | 17.91 | 1.388 | 1.38753646 | 0.00046354 | 24.85908 | 24.85077801 | 0.00830199 |
| 19 | 19.08 | 1.118 | 1.11843773 | 0.00043773 | 21.33144 | 21.33979183 | 0.00835183 |
| 20 | 21.02 | 0 | −0.0001509 | 0.00015090 | 0 | −0.00317188 | 0.00317188 |

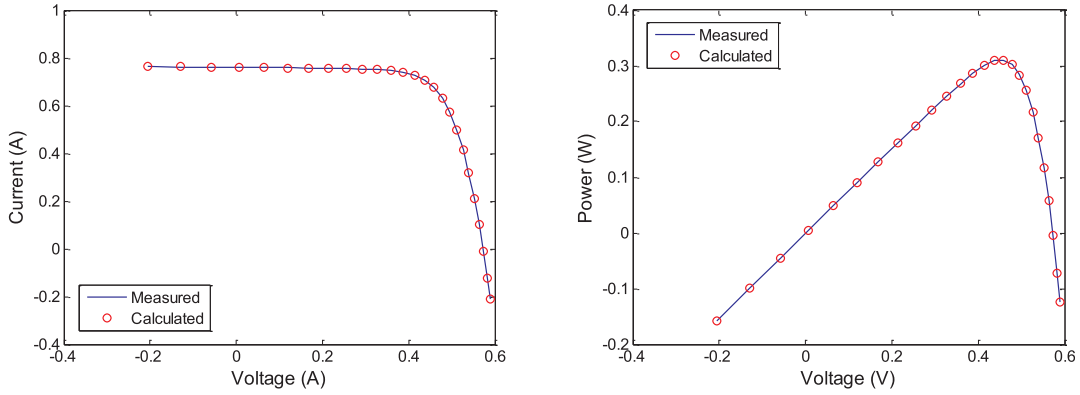


(a) I-V characteristic curve (b) P-V characteristic curve

**Fig. 6.** The measured data and calculated data obtained by GWOCS on single diode model.

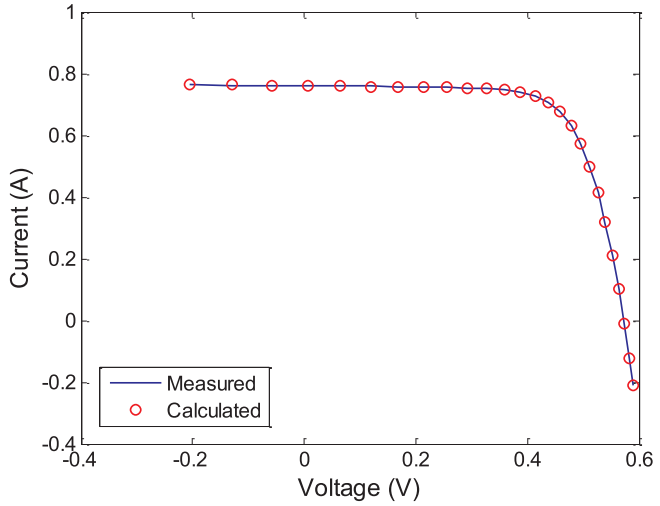


(a) I-V characteristic curve

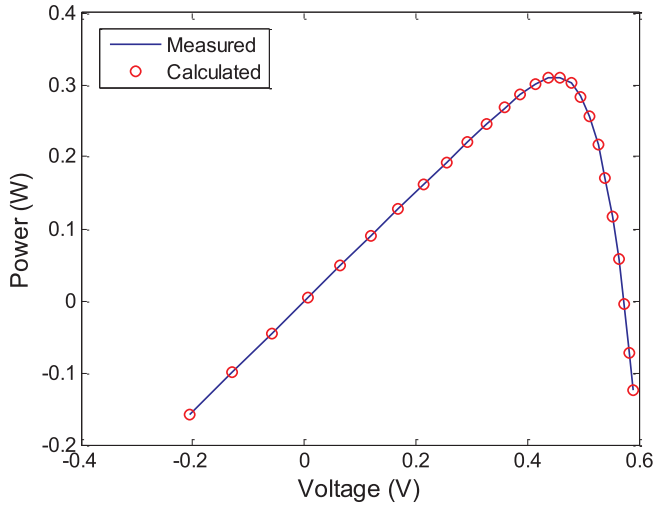


(b) P-V characteristic curve

**Fig. 7.** The measured data and calculated data obtained by GWOCS on double diode model.

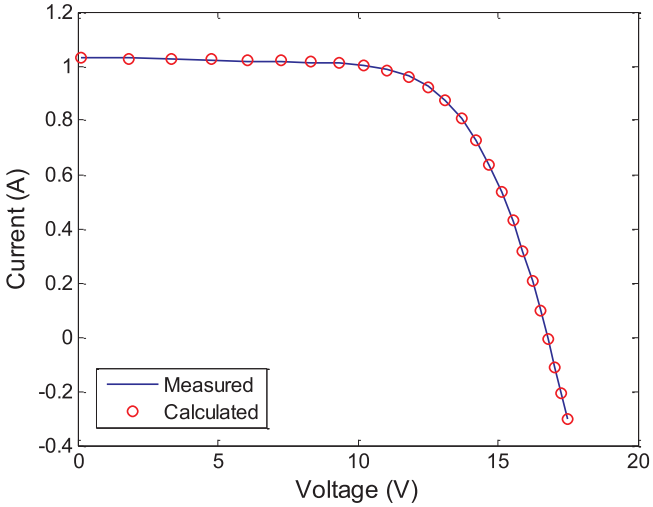


(a) I-V characteristic curve

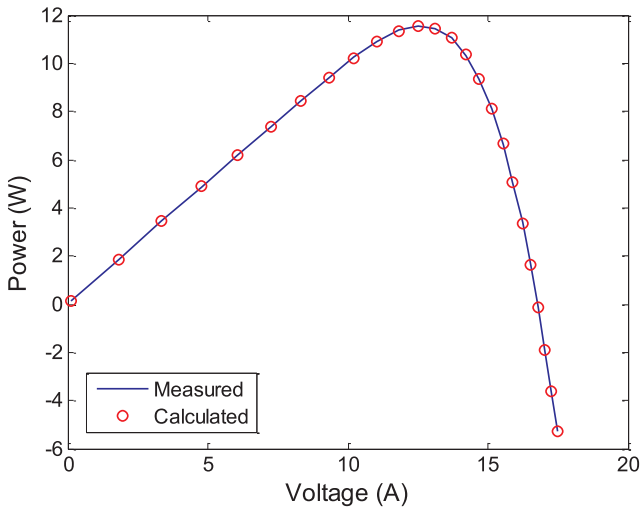


(b) P-V characteristic curve

**Fig. 8.** The measured data and calculated data obtained by GWOCS on Photowatt-PWP-201 module model.

$$\boldsymbol{X}_i = \begin{cases} \boldsymbol{X}_i + rand\cdot(\boldsymbol{X}_j - \boldsymbol{X}_k), & if \quad p > p_a \\ \boldsymbol{X}_i, & else \end{cases} \tag{17}$$

where $p \in [0, 1]$ is a random number, $\boldsymbol{X}_j$ and $\boldsymbol{X}_k$ are the candidate solutions from the population, respectively.

### 3.3. Opposition learning strategy

The GWO algorithm has been successfully applied to scientific and many engineering fields [67–69]. However, according to [62–64], the basic GWO algorithm is good at local exploitation, but poor at global exploration. Therefore, one active research topic is to enhance the global exploration ability of GWO. Opposition-based learning (OBL) strategy [70] is an effectively exploration-enhanced technique and has been widely applied meta-heuristic algorithms to strengthen their global exploration ability. The OBL strategy is explained as follows.

**Definition 1..** Opposite number. Considering a real number $x$, its opposite number $x'$ is defined as follows [70]:

$$x' = l + u - x \tag{18}$$

where $l$ and $u$ are the lower and upper boundary of $x$, respectively.

**Definition 2..** Opposite solution. The Eq. (18) can be extended to the $D$−dimensional search space. Assuming that $\boldsymbol{X} = (x_1, x_2, ...,x_D)$ is a solution in the $D$−dimensional search space. The opposite solution of $\boldsymbol{X}$ is defined as $\boldsymbol{X'} = (x_1', x_2', ...,x_D')$ [70]:

$$x_i' = l_i + u_i - x_i, \quad i = 1, 2, ...,D \tag{19}$$

Finally, the fitness function values of $f(\boldsymbol{X})$ and $f(\boldsymbol{X'})$ are calculated. If $f(\boldsymbol{X})$ is better than$f(\boldsymbol{X'})$, $\boldsymbol{X}$ is selected; otherwise, $\boldsymbol{X'}$ is selected.

More recently, the OBL strategy is applied to the GWO algorithm to improve its performance [71,72]. Different from References [71] and [72], this paper applies the OBL strategy for the decision layer individuals ($\alpha$, $\beta$, and $\delta$ wolves) with probability $p_b$ to further enhance the diversity of population.

### 3.4. Flow chart of GWOCS

The flow chart of GWOCS is shown in Fig. 4.

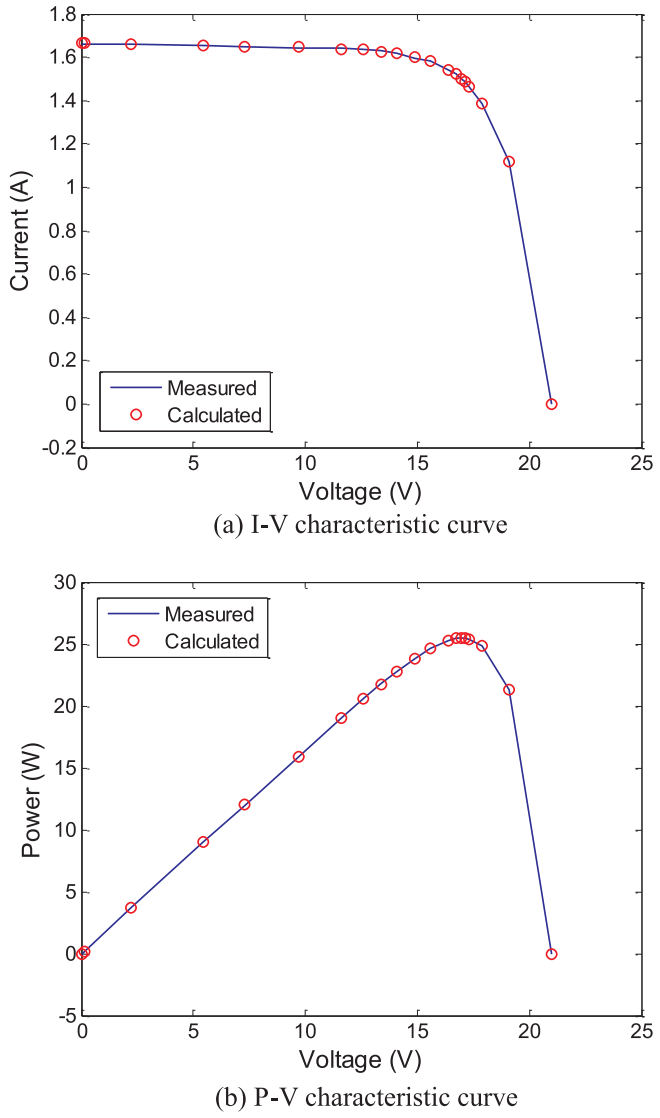


**Fig. 9.** The measured data and calculated data obtained by GWOCS on STM6-40/36 module model.

## 4. Results and analysis

### 4.1. GWOCS for benchmark test functions

In this subsection, 10 benchmark test functions are selected to verify the performance of GWOCS. The characteristics of these functions are provided in Table 1, where $f_1$-$f_4$ are unimodal, and $f_5$-$f_{10}$ are multimodal. The dimensions of each function are set to 30.

For comparison, the basic GWO algorithm [60], the modified GWO (mGWO) algorithm [73], and the enhanced GWO (EGWO) algorithm [74] are selected. In the subsection, the maximum number of iterations ($\max iter$) is used as the stopping condition. For four algorithms, the population size is 30 and the $\max iter$ set to 500. Moreover, 30 independent runs are conducted. All simulations are executed by MATLAB 2014a. Table 2 provided the mean and st.dev values obtained by four algorithms for 10 functions.

From Table 2, GWOCS obtained theoretical value (0) on all of the test functions except for $f_5(x)$. Compared with the basic GWO algorithm, GWOCS provides better "Mean" and "St.dev" values on all of the test functions. With respect to the mGWO and EGWO algorithms, GWOCS achieved better results on all of the test functions apart from $f_8(x)$. Table 3 provides the Friedman ranking of four algorithms. As can be seem in Table 3, the GWOCS obtained the first ranking, followed by mGWO, EGWO, and GWO.

Fig. 5 shows the convergence curves of the four compared algorithms on four typical functions. As can be seen from Fig. 5, the GWOCS achieved faster convergence and better accuracy than the other four compared algorithms on four typical functions.

### 4.2. GWOCS for parameter extraction of PV models

In order to further investigate the effectiveness of GWOCS, four different solar PV models parameter extraction problems are solved by GWOCS in this subsection. These models are the single diode, the double diode, the poly-crystalline Photowatt-PWP201 module, and the mono-crystalline STM6-40/36 module models, respectively. The I-V data of the single and double diode models is obtained by the 57 mm diameter commercial silicon R.T.C. France solar cell under 1000 W/m$^2$ at 33 °C [75]. The Photo-watt-PWP-201 and the STM6-40/36 modules are composed of 36 poly-crystalline and mono-crystalline cells connected in series and generate the I-V data under 1000 W/m$^2$ at 45 °C and 51 °C, respectively [9,75]. The search range of the parameters for the four PV models is listed in Table 4 [9,31,42,66].

To verify the performance of GWOCS, it is compared with seven well-known meta-heuristic algorithms, i.e., GWO [60], mGWO [73], EGWO [74], improved GWO (IGWO) [76], Alpha-guided GWO (AgGWO) [77], sine cosine algorithm (SCA) [78], and whale optimization algorithm (WOA) [79], as well as other reported results in the literature. For a fair comparison, GWOCS, GWO, mGWO, EGWO, IGWO, AgGWO, SCA, and WOA are set the same maximum number of function evaluations (i.e., Max_NFEs = 50,000). The other parameters settings of these seven algorithms are seen in their own literatures. All codes are programmed using MATLAB 2014a and each algorithm independently runs 30 times.

#### 4.2.1. Solution accuracy analysis

For the single diode, the double diode, the polycrystalline Photowatt-PWP201 module, and the mono-crystalline STM6-40/36 module models, the best extracted parameters and its corresponding RMSE values of GWOCS, GWO, mGWO, EGWO, IGWO, AgGWO, SCA, WOA and other reported results in the literatures are shown in Tables 5–8. It should be noted that the reported results in the literatures are directly derived from their corresponding papers.

From Table 5, for the single diode model, MADE, CS-BBO, BMO, CWOA, ISCA and TLBO-ABC algorithm obtained the best RMSE value (9.8602E − 04), while GWOCS provided the second best RMSE value (9.8607E − 04). The results of CS-BBO and TLBO-ABC indicated that the performance of the hybrid meta-heuristic algorithm was better than their own single algorithm. In addition, the maximum number of fitness evaluations (FEs) of BMO and CWOA were 30 and three times that of GWOCS, respectively. Compared with the remaining algorithms in Table 5, GWOCS achieved the better RMSE value.

As can be seen in Table 6, for the double diode model, ISCA algorithm achieved the best RMSE value (9.8237E − 04), while GWOCS obtained the fourth best RMSE value (9.8334E − 04). Compared with GWOCS, CS-BBO, BMO and CWOA algorithms provided the better RMSE values (9.8249E − 04, 9.8262E − 04 and 9.8272E − 04). However, the computational cost (i.e., number of FEs) of GWOCS was 1/3 and 1/30 that of BMO and CWOA, respectively. Moreover, GWOCS was superior to the remaining methods in Table 6 for the RMSE value.

Based on the results provided in Table 7, for the poly-crystalline Photowatt-PWP-201 module model, the performance of GWOCS was quite competitive compared with other approaches. GWOCS, MADE, TLBO-ABC, MLBSA, ISCA and MPCOA algorithms obtained the best RMSE value (2.4251E − 03). However, the MPCOA had the considerable maximum number of FEs (250000FEs), while the TLBO-ABC, MLBSA, and GWOCS had the minimum number of FEs (50000FEs). Compared with the remaining methods in Table 7, GWOCS obtained the better

**Table 13**
The statistical results of RMSE obtained by different algorithms for four models.

| Model | Algorithm | Min | Mean | Max | St.dev |
|---|---|---|---|---|---|
| Single diode model | GWO | 7.5011E−03 | 2.5617E−02 | 3.8160E−02 | 1.6071E−02 |
| | mGWO | 1.1278E−03 | 1.7220E−03 | 2.2054E−03 | 5.4732E−04 |
| | EGWO | 2.1121E−03 | 3.5015E−03 | 5.2490E−03 | 1.5988E−03 |
| | IGWO | 2.3038E−03 | 3.2492E−03 | 4.3283E−03 | 1.0188E−03 |
| | AgGWO | 6.7662E−03 | 6.9266E−03 | 7.1973E−03 | 2.3492E−04 |
| | SCA | 4.1410E−02 | 4.2862E−02 | 4.4145E−02 | 1.3754E−03 |
| | WOA | 3.2001E−03 | 1.8170E−02 | 3.7773E−02 | 1.7746E−02 |
| | GWOCS | **9.8607E−04** | **9.8874E−04** | **9.9095E−04** | **2.4696E−06** |
| Double diode model | GWO | 2.2124E−03 | 1.6222E−02 | 3.7996E−02 | 1.9113E−02 |
| | mGWO | 1.3163E−03 | 1.9078E−03 | 2.6602E−03 | 6.8622E−04 |
| | EGWO | 1.8062E−03 | 3.0670E−03 | 5.0069E−03 | 1.7050E−03 |
| | IGWO | 1.7576E−03 | 2.7192E−03 | 3.8871E−03 | 1.0796E−03 |
| | AgGWO | 1.1646E−03 | 1.4705E−02 | 3.8146E−02 | 2.0382E−02 |
| | SCA | 4.0585E−02 | 1.0180E−01 | 2.2286E−01 | 1.0485E−01 |
| | WOA | 3.1312E−03 | 4.5208E−03 | 5.4380E−03 | 1.2238E−03 |
| | GWOCS | **9.8334E−04** | **9.9411E−04** | **1.0017E−03** | **9.5937E−06** |
| Photowatt-PWP-201 module model | GWO | 2.6749E−03 | 3.4848E−03 | 4.0609E−03 | 7.2199E−04 |
| | mGWO | 2.6034E−03 | 3.5719E−03 | 5.2080E−03 | 1.4249E−03 |
| | EGWO | 2.6448E−03 | 3.7418E−03 | 4.4671E−03 | 9.6635E−04 |
| | IGWO | 2.6228E−03 | 4.5885E−03 | 7.2218E−03 | 2.3711E−03 |
| | AgGWO | 2.6145E−03 | 2.6172E−03 | 2.6193E−04 | 2.4404E−06 |
| | SCA | 3.1103E−02 | 1.9322E−01 | 2.7428E−01 | 1.4040E−01 |
| | WOA | 3.6253E−03 | 9.8291E−02 | 2.7425E−01 | 1.5253E−01 |
| | GWOCS | **2.4251E−03** | **2.4261E−03** | **2.4275E−03** | **1.1967E−06** |
| STM6-40/36 module model | GWO | 7.1412E−03 | 2.3733E−02 | 5.4215E−02 | 2.6432E−02 |
| | mGWO | 4.2511E−03 | 6.2544E−03 | 9.0403E−03 | 2.4887E−03 |
| | EGWO | 1.6458E−02 | 2.0803E−02 | 2.5667E−02 | 4.6262E−03 |
| | IGWO | 6.3448E−03 | 7.8755E−03 | 9.8971E−03 | 1.8263E−03 |
| | AgGWO | 5.8391E−03 | 8.7168E−03 | 1.1577E−02 | 2.8691E−03 |
| | SCA | 2.5407E−02 | 2.1564E−01 | 3.1077E−01 | 1.6475E−01 |
| | WOA | 7.5211E−03 | 2.0968E−01 | 3.1076E−01 | 1.7507E−01 |
| | GWOCS | **1.7337E−03** | **1.7457E−03** | **1.7528E−03** | **1.0447E−05** |

**Table 14**
Ranking of the GWOCS and other compared algorithms on four PV models according to the Friedman test.

| Algorithm | Friedman ranking | Final ranking |
|---|---|---|
| GWO | 5.75 | 6 |
| mGWO | 2.50 | 2 |
| EGWO | 4.50 | 5 |
| IGWO | 3.75 | 3 |
| AgGWO | 4.25 | 4 |
| SCA | 8.00 | 8 |
| WOA | 6.25 | 7 |
| GWOCS | 1.00 | 1 |

RMSE value.

With respect to the results listed in Table 8, for the mono-crystalline STM6-40/36 module model, ITLBO and CS-BBO algorithms obtained the best RMSE value (1.7298E−03), followed by GWOCS, TLBO-ABC, TBLO, CS, BLPSO, GWO, ABC, AgGWO, IGWO, mGWO, WOA, EGWO, and SCA.

After extracting the model parameters, the output current and power corresponding to the measured voltage can be easily calculated. To further show the accuracy of GWOCS, Tables 9–12 listed the calculated values of output current and power as well as the individual absolute error (IAE), respectively. Moreover, Figs. 6–9 provide the I-V and P-V characteristic curves for four PV models.

As can be seen from Tables 6–9, for the single diode, the double diode, the Photowatt-PWP-201 module, and the STM6-40/36 module models, the all IAE values of current are not more than 0.00159097, 0.00159294, 0.00439919, and 0.00593106, respectively and the all IAE values of power are less than 0.00101275, 0.00080741, 0.04388388, and 0.08825422, respectively. Additionally, the I-V and P-V characteristic curves of the four extracted models in Figs. 6–9 show that the calculated data obtained by GWOCS are highly match the measured data. The results in Tables 9–12 and Figs. 6–9 indicate that GWOCS has better accuracy than most algorithms for four solar PV models.

#### 4.2.2. Robustness and statistics analysis

To further investigate the robustness and reliability of GWOCS, the statistical results obtained by GWO, mGWO, EGWO, IGWO, AgGWO, SCA, WOA, and GWOCS algorithms for the single diode, the double diode, the Photowatt-PWP-201 module, and the STM6-40/36 module models are listed in Table 13. These results include the minimum RMSE (min), the maximum RMSE (max), the mean RMSE (mean), and the standard deviation of RMSE (St.dev) values. The best statistical results of each model are shown in bold. In addition, the Friedman ranking test results of GWOCS and the other compared algorithms for four PV models are provided in Table 14.

From Table 13, GWOCS performs significantly better than the GWO, mGWO, EGWO, IGWO, AgGWO, SCA, and WOA algorithms on the single diode, the double diode, the Photowatt-PWP-201 module, and the STM6-40/36 module models. The statistical results in Table 13 show that GWOCS is the most reliable and stable parameter identification technique.

As shown from Table 14, according to the Friedman ranking test, the best ranking obtained by GWOCS, followed by mGWO, IGWO, AgGWO, EGWO, GWO, WOA, and SCA.

Moreover, Fig. 10 provides the boxplot of GWO, mGWO, EGWO, IGWO, AgGWO, SCA, WOA, and GWOCS algorithms for the single diode, the double diode, the Photowatt-PWP-201 module, and the STM6-40/36 module models, which displays the distribution of results obtained by different algorithms in 30 runs.

Based on the comparisons on the solution distribution in Fig. 10, it can be observed that the proposed GWOCS algorithm shows the best performance compared with other seven algorithms in terms of

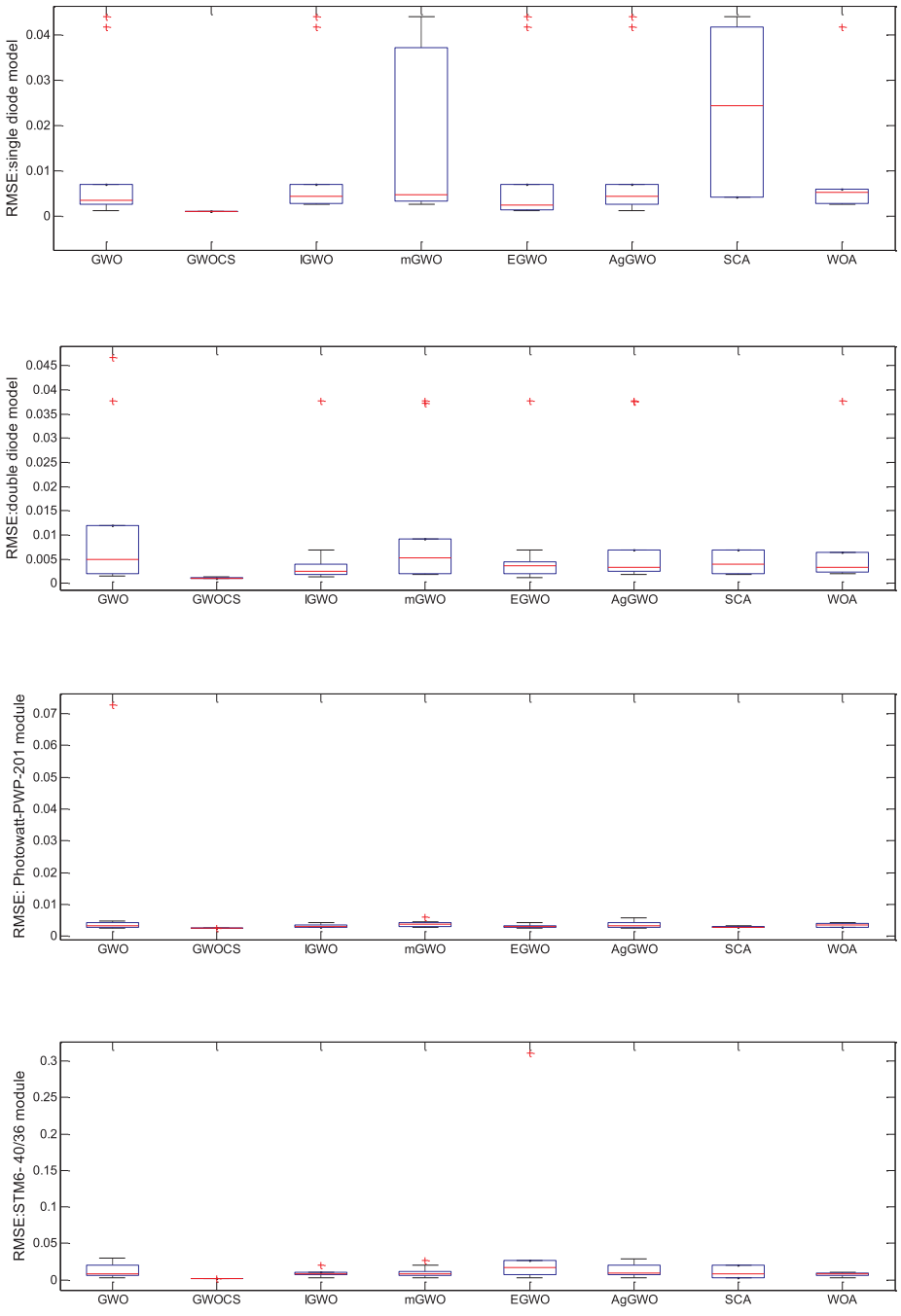


**Fig. 10.** Boxplot of best RMSE in 30 runs for four different PV models.

accuracy and robustness.

#### 4.2.3. Convergence analysis

To investigate the computational efficiency of GWOCS, Fig. 11 plots the convergence curves of four PV models obtained by GWO, mGWO, EGWO, IGWO, AgGWO, SCA, WOA, and GWOCS with the same number of fitness evaluations (FEs), i.e., 50000.

As can be seem in Fig. 11, for the single diode, the double diode, the Photowatt-PWP-201 module, and the STM6-40/36 module models, GWOCS obtained faster convergence speed and higher solution precision than the other compared algorithms.

## 5. Conclusion

In this paper, a new hybridization of grey wolf optimizer and cuckoo search (GWOCS) is developed to solve the global optimization problems and extract the parameters of several solar PV cell models under different operating conditions. To the best of our knowledge, it is the first attempt to design a hybrid algorithm based on GWO and CS for extracting the parameters of PV models. The cooperation of the two metaheuristic algorithms can achieve an efficient balance between exploration and exploitation. In addition, GWOCS utilizes the opposition-based learning strategy for the decision layer individuals to further enhance the diversity of population. GWOCS is applied to solve ten global optimization problems with different characteristics and four solar PV models parameters extraction problems, i.e., the single diode, double diode, Photowatt-PWP-201 module, and the STM6-40/36 module models. The conclusions based on the experimental results are summarized as follows:

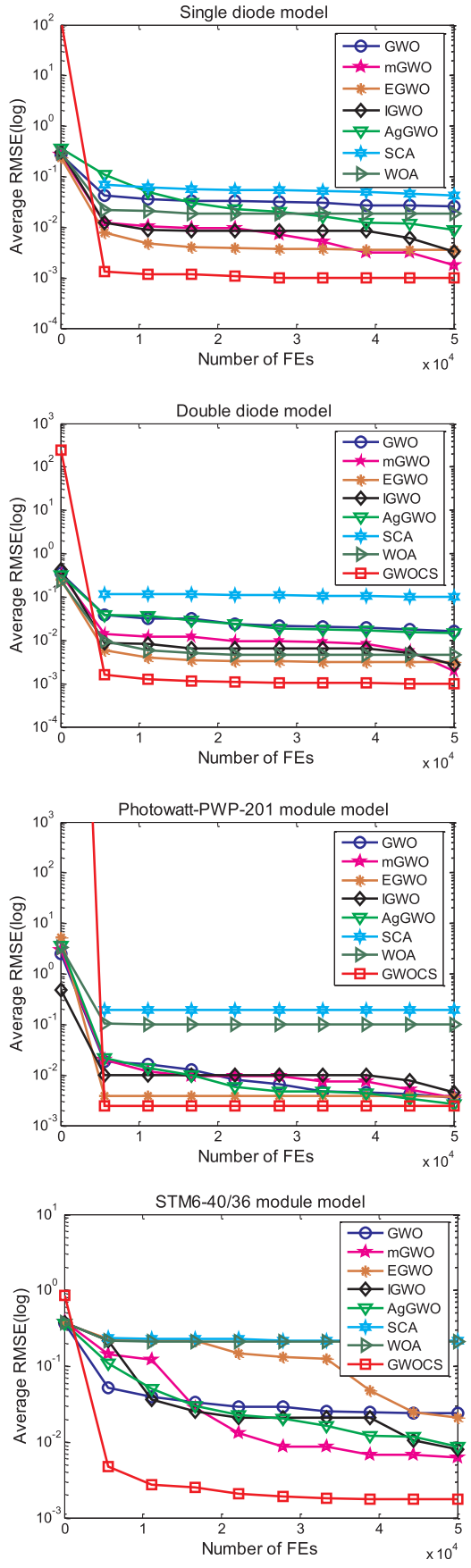


**Fig. 11.** Convergence curves of GWOCS and other seven algorithms for four PV models.

1) The solution precision and convergence speed of global optimization problems show that GWOCS has better performance than other algorithms such as GWO, EGWO, and mGWO.
2) According to the solution accuracy results, the IAE results, the Friedman ranking test results, the I-V and the P-V characteristic curves, GWOCS displays better or similar performance on four different solar PV cell models than the other compared approaches.
3) The statistical results demonstrate that GWOCS has better robustness on parameter extraction problem of four PV models.
4) The convergence curves indicate that GWOCS has faster convergence speed than other compared algorithms.

These conclusions confirm that GWOCS is a promising candidate technique for extracting the parameters of solar PV models. For future studies, utilizing GWOCS to handle the other energy optimization problems such as optimal configuration of distributed generation, energy scheduling, and economic load dispatch problem is also very interesting.

## Declaration of Competing Interest

The authors declare that they have no known competing financial interests or personal relationships that could have appeared to influence the work reported in this paper.

## Acknowledgments

This work was partly support by the National Natural Science Foundation of China under Grant No. 61463009, the Science and Technology Top Talents of Higher Learning Institutions of Guizhou Province under Grant No. KY[2017]070, and the Science and Technology Foundation of Guizhou Province under Grant No. [2016] 1022.

## References

[1] Ayala HVH, Santos Coelho L, Mariani VC, Askarzadeh A. An improved free search differential evolution algorithm: a case study on parameter identification of one diode equivalent circuit of a solar cell module. Energy 2015;93:1515–22.
[2] Li S, Gong W, Yan X, Hu C, Bai D, Wang L, et al. Parameter extraction of photovoltaic models using an improved teaching-learning-based optimization. Energy Convers Manage 2019;186:293–305.
[3] Yeh WC, Huang CL, Lin P, Chen Z, Jiang Y, Sun B. Simplex simplified swarm optimization for the efficient optimization of parameter identification for solar cell models. IET Renew Power Generat 2018;12(1):45–51.
[4] Batzelis EI, Kampitsis GE, Papathanassiou SA, Manias SN. Direct MPP calculation in terms of the single-diode PV model parameters. IEEE Trans Energy Convers 2015;30:226–36.
[5] Chin VJ, Salam Z, Ishaque K. Cell modelling and model parameters estimation techniques for photovoltaic simulator application: a review. Appl Energy 2015;154:500–19.
[6] Jordehi AR. Time varying acceleration coefficients particle swarm optimization (tvacpso): a new optimization algorithm for estimation parameters of pv cells and modules. Energy Convers Manage 2016;129:262–74.
[7] Chin VJ, Salam Z, Ishaque K. An accurate modeling of the two-diode model of PV module using a hybrid solution based on differential evolution. Energy Convers Manage 2016;124:42–50.
[8] Gao X, Cui Y, Hu J, Xu G, Wang Z, Qu J, et al. Parameter extraction of solar cell models using improved shuffled complex evolution algorithm. Energy Convers Manage 2018;157:460–79.
[9] Gnetchejo PJ, Essiane SN, Ele P, Wamkeue R, Wapet DM, Ngoffe SP. Important notes on parameter estimation of solar photovoltaic cell. Energy Convers Manage 2019;197:111870.
[10] Chin VJ, Salam Z, Ishaque K. Cell modeling and model parameters estimation techniques for photovoltaic simulator application: a review. Appl Energy 2015;154:500–19.
[11] Awadallah MA. Variations of the bacterial foraging algorithm for the extraction of PV module parameters from nameplate data. Energy Convers Manage 2016;113:312–20.
[12] Peng L, Sun Y, Meng Z, Wang Y, Xu Y. A new method for determining the characteristics of solar cells. J Power Sources 2013;227:131–6.
[13] Fathabadi H. Novel neural-analytical method for determining silicon/plastic solar cells and modules characteristics. Energy Convers Manage 2013;76:253–9.
[14] Chen Y, Wang X, Li D, Hong R, Shen H. Parameters extraction from commercial solar cells I-V characteristics and shunt analysis. Appl Energy 2011;88(6):2239–44.

[15] El Tayyan AA. An approach to extract the parameters of solar cells from their illuminated I-V curves using the Lambert W function. Turkish J Phys 2015;39:1–15.
[16] Gao X, Cui Y, Hu J, Xu G, Yu Y. Lambert W-function based exact representation for double diode model of solar cells: comparison on fitness and parameter extraction. Energy Convers Manage 2016;127:443–60.
[17] Chan DSH, Phang JCH. Analytical methods for the extraction of solar-cell single- and double-diode model parameters from I-V characteristics. IEEE Trans Electron Dev 1987;34(2):286–93.
[18] Sandrolini L, Artioli M, Reggiani U. Numerical method for the extraction of photovoltaic module double-diode model parameters through cluster analysis. Appl Energy 2010;87:442–51.
[19] Kler D, Goswami Y, Rana KPS, Kumar V. A novel approach to parameter estimation of photovoltaic systems using hybridized optimizer. Energy Convers Manage 2019;187:486–511.
[20] Oliva D, Elaziz MA, Elsheikh AH, Ewees AA. A review on meta-heuristics methods for estimating parameters of solar cells. J. Power Sources 2019;435:126683.
[21] Balasubramanian K, Jacob B, Priya K, Sangeetha K, Rajasekar N, Babu TS. Critical evaluation of genetic algorithm based fuel cell parameter extraction. Energy Proc 2015;75:1975–82.
[22] Ismail M, Moghavvemi M, Mahlia T. Characterization of PV panel and global optimization of its model parameters using genetic algorithm. Energy Convers Manage 2013;73:10–25.
[23] Jordehi AR. Enhanced leader particle swarm optimization (ELPSO): An efficient algorithm for parameter estimation of photovoltaic (PV) cells and modules. Sol Energy 2018;159:78–87.
[24] Nunes HGG, Pombo JAN, Mariano SJPS. Calado MRA, Felippe de Souza JAM. A new high performance method for determining the parameters of PV cells and modules based on guaranteed convergence particle swarm optimization. Appl Energy 2018;211:774–91.
[25] Yousri D, Allam D, Eteiba MB, Suganthan PN. Static and dynamic photovoltaic models' parameters identification using chaotic heterogeneous comprehensive learning particle swarm optimizer variants. Energy Convers Manage 2019;182:546–63.
[26] Ishaque K, Salam Z, Mekhilef S, Shamsudin A. Parameter extraction of solar photovoltaic modules using penalty-based differential evolution. Appl Energy 2012;99:297–308.
[27] Elaziz MA, Oliva D. Parameter estimation of solar cells diode models by an improved opposition-based whale optimization algorithm. Energy Convers Manage 2018;171:1843–59.
[28] Li S, Gong W, Yan X, Hu C, Bai D, Wang L. Parameter estimation of photovoltaic models with memetic adaptive differential evolution. Sol Energy 2019;190:465–74.
[29] Chen X, Yu K. Hybridizing cuckoo search algorithm with biogeography-based optimization for estimating photovoltaic model parameters. Sol Energy 2019;180:192–206.
[30] Oliva D, Cuevas E, Pajares G. Parameter identification of solar cells using artificial bee colony optimization. Energy 2014;72:93–102.
[31] Chen X, Xu B, Mei C, Ding Y, Li K. Teaching-learning- based artificial bee colony for solar photovoltaic parameter estimation. Appl Energy 2018;212:1578–88.
[32] Rajasekar N, Kumar NK, Venugopalan R. Bacterial foraging algorithm based solar PV parameter estimation. Sol Energy 2013;97:255–65.
[33] Subudhi B, Pradhan R. Bacterial foraging optimization approach to parameter extraction of a photovoltaic module. IEEE Trans Sustain Energy 2018;9:381–9.
[34] Niu Q, Zhang L, Li K. A biogeography-based optimization algorithm with mutation strategies for model parameter estimation of solar and fuel cells. Energy Convers Manage 2014;86:1173–85.
[35] Alam DF, Yousri DA, Eteiba MB. Flower pollination algorithm based solar PV parameter estimation. Energy Convers Manage 2015;101:410–22.
[36] Xu S, Wang Y. Parameter estimation of photovoltaic modules using a hybrid flower pollination algorithm. Energy Convers Manage 2017;114:53–68.
[37] Yu K, Liang J, Qu B, Chen X, Wang H. Parameters identification of photovoltaic models using an improved JAYA optimization algorithm. Energy Convers Manage 2017;150:742–53.
[38] Yu K, Qu B, Yue C, Ge S, Chen X, Liang J. A performance guided JAYA algorithm for parameters identification of photovoltaic cell and module. Appl Energy 2019;237:241–57.
[39] Abbassi R, Abbassi A, Heidari AA, Miajalili S. An efficient salp swarm-inspired algorithm for parameters identification of photovoltaic cell models. Energy Convers Manage 2019;179:362–72.
[40] Askarzadeh A, Coelho LS. Determination of photovoltaic modules parameters at different operating conditions using a novel bird mating optimizer approach. Energy Convers Manage 2015;89:608–14.
[41] Patel SJ, Panchal AK, Kheraj V. Extraction of solar cell parameters from a single current-voltage characteristic using teaching learning based optimization algorithm. Appl Energy 2014;119:384–93.
[42] Yu K, Chen X, Wang X, Wang Z. Parameters identification of photovoltaic models using self-adaptive teaching-learning-based optimization. Energy Convers Manage 2017;145:233–46.
[43] Chen X, Yu K, Du W, Zhao W, Liu G. Parameters identification of solar cell models using generalized oppositional teaching learning based optimization. Energy 2016;99:170–80.
[44] Yu K, Liang J, Qu B, Cheng Z, Wang H. Multiple learning backtracking search algorithm for estimating parameters of photovoltaic models. Appl Energy 2018;226:408–22.
[45] Oliva D, Aziz MAE, Hassanien AE. Parameter estimation of photovoltaic cells using an improved chaotic whale optimization algorithm. Appl Energy 2017;200:141–54.
[46] Chen H, Jiao S, Heidari AA, Wang M, Chen X, Zhao X. An opposition-based sine cosine approach with local search for parameter estimation of photovoltaic models. Energy Convers Manage 2019;195:927–42.
[47] Fathy A, Rezk H. Parameter estimation of photovoltaic system using imperialist competitive algorithm. Renew Energy 2017;111:307–20.
[48] Ali EE, El-Hameed MA, El-Fergany AA, El-Arini MM. Parameter extraction of photovoltaic generating units using multi-verse optimizer. Sustain Energy Tech Assess 2016;17:68–76.
[49] Wu Z, Yu D, Kang X. Parameter identification of photovoltaic cell model based on improved ant lion optimizer. Energy Convers Manage 2017;151:107–15.
[50] Guo L, Meng Z, Sun Y, Wang L. Parameter identification and sensitivity analysis of solar cell models with cat swarm optimization algorithm. Energy Convers Manage 2016;108:520–8.
[51] Askarzadeh A, Rezazadeh A. Parameter identification for solar cell models using harmony search-based algorithms. Sol Energy 2012;86:3241–9.
[52] Beigi AM, Maroosi A. Parameter identification for solar cells and module using a hybrid firefly and pattern search algorithm. Sol Energy 2018;171:435–46.
[53] Lin P, Cheng S, Yeh W, Chen Z, Wu L. Parameters extraction of solar cell models using a modified simplified swarm optimization algorithm. Sol Energy 2017;144:594–603.
[54] Allam D, Yousri DA, Eteiba MB. Parameters extraction of the three diode model for the multi-crystalline solar cell/ module using moth-flame optimization algorithm. Energy Convers Manage 2016;123:535–48.
[55] Chen Z, Wu L, Lin P, Wu Y, Cheng S. Parameters identify-cation of photovoltaic models using hybrid adaptive Nelder-Mead simplex algorithm based on eagle strategy. Appl Energy 2016;182:47–57.
[56] Kler D, Sharma P, Banerjee A, Rana KPS, Kumar V. PV cell and module efficient parameters estimation using evaporation rate based water cycle algorithm. Swarm Evol Comput 2017;35:93–110.
[57] Rezk H, Fathy A. A novel optimal parameters identification of triple-junction solar cell based on a recently meta-heuristic water cycle algorithm. Sol Energy 2017;157:778–91.
[58] Hasanien HM. Shuffled frog leaping algorithm for photo-voltaic model identification. IEEE Trans Sustain Energy 2015;6:509–15.
[59] Xiong G, Zhang J, Yuan X, Shi D, He Y, Yao G. Parameter extraction of solar photovoltaic models by means of a hybrid differential evolution with whale optimization algorithm. Sol Energy 2018;176:742–61.
[60] Mirjalili S, Mirjalili SM, Lewis A. Grey wolf optimizer. Adv Eng Softw 2014;69:46–61.
[61] Yang X, Deb S. Cuckoo search via levy flights. World congress on nature & biologically inspired computing. IEEE; 2009. p. 210–4.
[62] Long W, Jiao J, Liang X, Tang M. An exploration-enhanced grey wolf optimizer to solve high-dimensional numerical optimization. Eng Appl Artif Intell 2018;68:63–80.
[63] Saxena A, Kumar R, Das S. $\beta$-Chaotic map enabled grey wolf optimizer. Appl Soft Comput 2019;75:84–105.
[64] Gupta S, Deep K. A novel random walk grey wolf optimizer. Swarm Evol Comput 2019;44:101–12.
[65] Mlakar U, Fister Jr. I. Hybrid self-adaptive cuckoo search for global optimization. Swarm Evol Comput 2016;29:47–72.
[66] Gong W, Cai Z. Parameter extraction of solar cell models using repaired adaptive differential evolution. Sol Energy 2013;94:209–20.
[67] Long W, Jiao J, Liang X, Tang M. Inspired grey wolf optimizer for solving large-scale function optimization problems. Appl Math Model 2018;60:112–26.
[68] Martin B, Marot J, Bourennane S. Mixed grey wolf optimizer for the joint denoising and unmixing of multi-spectral images. Appl Soft Comput 2019;74:385–410.
[69] Singh D, Dhillon JS. Ameliorated grey wolf optimization for economic load dispatch problem. Energy 2019;169:398–419.
[70] Tizhoosh HR. Opposition-based learning: a new scheme for machine intelligence. Int Conf Comput Intell Model Control Auto 2005;1:695–701.
[71] Ibrahim RA, Elaziz MA, Lu S. Chaotic opposition-based grey wolf optimization algorithm based on differential evolution and disruption operator for global optimization. Expert Syst Appl 2018;108:1–27.
[72] Guha D, Roy PK, Banerjee S. Load frequency control of large scale power system using quasi-oppositional grey wolf optimization algorithm. Eng Sci Technol 2016;19:1693–713.
[73] Mittal N, Singh U, Sohi BS. Modified grey wolf optimizer for global engineering optimization. Appl Comput Intell Soft Comput 2016;2016:1–16.
[74] Joshi H, Arora S. Enhanced grey wolf optimization algorithm for global optimization. Fundam Inform 2017;153:235–64.
[75] Easwarakhanthan T, Bottin J, Bouhouch I, Boutrit C. Nonlinear minimization algorithm for determining the solar cell parameters with microcomputers. Int J Sol Energy 1986;4:1–12.
[76] Long W, Liang X, Cai S, Jiao J, Zhang W. A modified augmented Lagrangian with improved grey wolf optimization to constrained optimization problems. Neural Comput Appl 2017;28:421–38.
[77] Hu P, Chen S, Huang H, Zhang G, Liu L. Improved alpha-guided grey wolf optimizer. IEEE Access 2019;7:5421–37.
[78] Mirjalili S. SCA: a sine cosine algorithm for solving optimization problems. Knowl-Based Syst 2016;96:120–33.
[79] Mirjalili S, Lewis A. The whale optimization algorithm. Adv Eng Softw 2016;95:51–67.
[80] El-Naggar KM, Alrashidi MR, Alhajri MF, Al-Othman AK. Simulated annealing algorithm for photovoltaic parameter identification. Sol Energy 2012;86:266–74.
[81] Yuan X, Xiang Y, He Y. Parameter extraction of solar cell models using mutative-scale parallel chaos optimization algorithm. Sol Energy 2014;108:238–51.